

The emergence of a globally productive biosphere

Rogier Braakman^{1,2}

¹ Department of Civil and Environmental Engineering,

² Department of Earth, Atmospheric and Planetary Sciences, Massachusetts Institute of Technology, Cambridge, MA, USA

Corresponding Author:

Rogier Braakman

Email address: rogierbraakman@gmail.com

The emergence of a globally productive biosphere

Rogier Braakman^{1,2,*}

Departments of ¹Civil & Environmental Engineering and ²Earth, Atmospheric & Planetary Science,
Massachusetts Institute of Technology. *E-mail: rogiembraakman@gmail.com

Abstract

A productive biosphere and oxygenated atmosphere are defining features of Earth and are fundamentally linked. Here I argue that cellular metabolism imposes central constraints on the historical trajectories of biospheric productivity and atmospheric oxygenation. Photosynthesis depends on iron, but iron is highly insoluble under the aerobic conditions produced by oxygenic photosynthesis. These counteracting constraints led to two major stages of biospheric expansion and Earth oxygenation. Near the Archean-Proterozoic boundary, cyanobacterial photosynthesis expanded in shallow aquatic environments and along the edges of continents, where weathering inputs made iron more easily accessible. The anoxic deep open ocean was rich in free iron, but this iron remained effectively inaccessible since a photosynthetic expansion would have quenched its own supply. Near the Proterozoic-Phanerozoic boundary, major bioenergetic innovations allowed eukaryotic photosynthesis to begin expanding out into the deep open ocean and onto the continents, eventually creating a globally productive biosphere. These arguments emerge from a recent reconstruction of metabolic evolution in marine *Synechococcus* and *Prochlorococcus*, abundant marine picocyanobacteria whose ancestors colonized the oceans in the Neoproterozoic. This reconstruction revealed a sequence of innovations that ultimately produced a form of photosynthesis in *Prochlorococcus* that is more like that of green plant cells than other cyanobacteria. Innovations increased the energy flux of cells, thereby enhancing their ability to acquire sparse nutrients, and as a by-product increased production of iron-chelating organic carbon. This pushed the oceans through a transition from an anoxic state rich in free iron to an oxygenated state with organic carbon-bound iron. In addition to major increases in biospheric productivity, both the Neoproterozoic and Neoproterozoic have also been linked to global glaciations, major carbon cycle perturbations and changes in the nature of mantle convection and plate tectonics. This suggests the dynamics of life and Earth are intimately intertwined across levels and that similar general principles governed Neoproterozoic and Neoproterozoic transitions in these coupled dynamics.

Introduction

The oxygenation of Earth's atmosphere is the result of a complex interplay of geological and biological forces, and untangling these forces is a major scientific challenge. The ultimate source of oxygen is oxygenic photosynthesis, which is coupled to aerobic respiration as part of the biological carbon cycle (Fig. 1). However, if photosynthesis and respiration were perfectly coupled oxygen could not accumulate, and it is generally thought that the long-term sequestration of a small fraction (~0.1%) of the organic carbon produced by photosynthesis within Earth's subsurface is responsible for the rise of atmospheric oxygen [1-5]. Buried organic carbon eventually returns to the atmosphere as CO₂ when organic-bearing rocks are exhumed and oxidatively weathered, or when metamorphism during subduction leads to outgassing of CO₂ or reduced gasses, the latter of which can react with O₂ (Fig. 1) [2,6]. A potentially critical process that is less constrained is the subduction of organic carbon into the mantle, from where its recycling to the surface is slower than

48 crustal recycling [2,7-12]. In this view of the carbon cycle (Fig. 1), an increase in the *steady state*
 49 atmospheric oxygen levels is thus linked to increase in the *steady state* organic carbon content of
 50 Earth's crust and/or mantle. Changes in abiotic sinks for O₂ other than outgassing of reducing
 51 power derived directly from buried organic carbon, for example due to redox changes in the
 52 mantle, crust and/or volcanic gasses, have also been argued to be important contributing processes
 53 [13-18].
 54

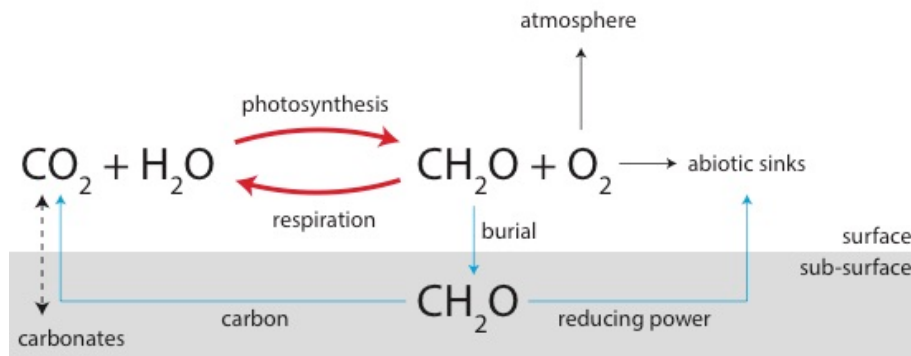


Figure 1. Simplified view of the coupled biological (red) and geological (blue) cycles of organic carbon and associated reducing power and their relationship to atmospheric oxygen. Oxygenic photosynthesis produces organic carbon (represented in its general stoichiometry of CH₂O) and oxygen from CO₂ and water, while aerobic respiration performs the reverse process. A small fraction (~0.1%) of organic carbon escapes oxidation through sequestration in sediments, allowing oxygen to accumulate in the atmosphere over geologic time. Geologic processes in the crust and mantle eventually recycle the carbon and reducing power within buried organic carbon back to the surface. The organic carbon cycle is ultimately tied to the inorganic carbon cycle (shown as bidirectional arrows between CO₂ and carbonates), further linking the evolution of the biosphere and the solid Earth.

55 There are generally considered to be two major stages of Earth oxygenation. The first stage, also
 56 known as the ‘Great Oxidation Event’ [14], occurred near the boundary between the Archean
 57 (4000-2500 Mya) and Proterozoic (2500-541 Mya) and is when the atmosphere first became
 58 permanently oxygenated at around 0.1-1% of modern levels [1,19-25]. After a prolonged period
 59 of relative global stasis [26-28], atmospheric oxygen restarted its climb toward modern levels near
 60 the boundary between the Proterozoic and Phanerozoic (541 Mya – current), eventually increasing
 61 an additional 2-3 orders of magnitude and paving the way for the rise of large multi-cellular
 62 animals [29-37]. In this review I will focus on this second stage, also known as the ‘Neoproterozoic
 63 Oxidation Event’ [37], and in particular on metabolic innovations occurring in the oceanic
 64 biosphere at that time.
 65

66 The basic relationship between the global carbon cycle and atmospheric oxygen (Fig. 1) suggests
 67 that understanding the balance between primary production and aerobic respiration, and the
 68 resulting impact on carbon burial, is key to understanding the history of Earth oxygenation. It has
 69 previously been argued that Neoproterozoic (1000-541 Mya) oxygenation may have been driven
 70 by effective decreases in the efficiency of respiration due to faster sinking of larger organisms
 71 and/or their fecal pellets [38-41] or because of changes in the composition sediments that more
 72 efficiently trapped organic matter [42,43]. I will focus on possible sources of variation in global
 73 rates of photosynthesis, which is ultimately the source flux of both oxygen and the carbon whose
 74 burial allows accumulation of oxygen. While all oxygenic photosynthesis is performed by
 75 cyanobacteria or photosynthetic eukaryotes (whose chloroplasts are derived from cyanobacteria),

76 each of these broad groups contain a great diversity of lineages that have different physiologies,
77 occupy different ecological niches and which arose at different times in Earth history [44-47].
78 Identifying the driving forces that underpin the evolutionary diversification of oxygenic
79 photosynthesizers is important for understanding the evolution of the carbon cycle (Fig. 1).

80
81 Broadly speaking, the Neoproterozoic is when photosynthetic eukaryotes began to take over from
82 cyanobacteria as the dominant primary producers, eventually driving a major increase in global
83 primary production [48-55]. Important exceptions that ultimately help explain this “rule” are the
84 marine picocyanobacteria *Synechococcus* and *Prochlorococcus* [56-59], whose ancestors also
85 arose in the Neoproterozoic [60,61] and which are estimated to account for around 25% of
86 biological CO₂-fixation in the modern oceans [62]. We recently reconstructed the metabolic
87 evolution of this group [63], which revealed key evolutionary driving forces and biogeochemical
88 feedbacks that help us understand both the long-term oxygenation of the oceans as well as the
89 general ecological dominance of photosynthetic eukaryotes. To place observed metabolic
90 innovations in context, I will first review the evolution of ocean chemistry between the
91 Neoproterozoic and early Phanerozoic.

92 93 Biogeochemical dynamics of the Neoproterozoic and early Phanerozoic

94
95 Marine picocyanobacteria expanded into the oceans during a time of major upheaval in the whole
96 Earth system. Geologic records from the period bridging the Neoproterozoic and early Phanerozoic
97 indicate the breakup of the super-continent Rodinia [64-67], possible changes in the nature of plate
98 tectonics linked to cooling of the mantle and crust [68-74], an expansion of shallow seas [66,75-
99 77], major carbon cycle perturbations [38,78,79] and several “snowball Earth” episodes of global
100 glaciation [80-83]. At the same time, ocean chemistry was undergoing a fundamental shift (Fig.
101 2). It has in recent decades become increasingly clear that the deep open ocean remained largely
102 anoxic well into the Proterozoic, long after oxygen first began accumulating in the atmosphere
103 [84]. It was first thought that Proterozoic oceans were mostly euxinic (rich in H₂S) [84], but more
104 recent evidence suggests the oceans were instead largely ferruginous (rich in Fe²⁺) [85,86], with
105 euxinia restricted to regions of enhanced productivity near continental boundaries [26,87]. In
106 contrast, the modern oceans are largely oxygenated. The exact time course of ocean oxygenation
107 is actively being debated – recent evidence suggests the oceans may not have become permanently
108 oxygenated until the early Ordovician (ca. 400 Mya) [88] or even the Triassic (ca. 200 Mya) [89]
109 – but evidence for the initiation of this process reaches back to the Neoproterozoic [35,88-92].

110
111 Several biogeochemical feedbacks have been proposed to explain why the deep open ocean
112 remained anoxic during the Proterozoic. Some proposals invoke nitrogen-limitation of oceanic
113 primary production, either through the scavenging of Molybdenum and other trace metals that
114 mediate nitrogen assimilation by sulfide ions in euxinic waters [50,26], or due to an excess in the
115 rate of denitrification relative to nitrification under low oxygen concentrations [93] (Fig. 2). Other
116 proposals invoke phosphorus-limitation of primary production, due to the scavenging of phosphate
117 from riverine inputs and/or directly from the water column by abundant Fe²⁺ ions [94-97], or due
118 to organic phosphate remineralization being limited by electron acceptors in the absence of O₂
119 [98]. Both sets of proposals are consistent with observations that post-Neoproterozoic oceans saw
120 significant increases in the levels of both phosphate [97,99] and molybdenum [90,100], as well as
121 isotopic shifts of sedimentary nitrogen that suggest the onset of a stable oceanic nitrate pool [101-

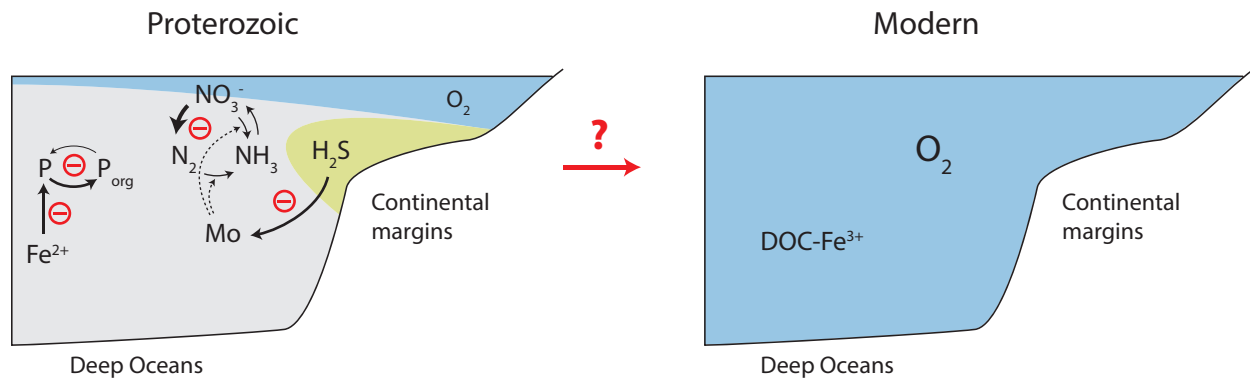


Figure 2. Neoproterozoic revolution in ocean chemistry. Negative feedbacks that have been argued to constrain ocean oxygenation are indicated with red minus signs. Processes that scavenge phosphorus [94-97] and/or molybdenum (Mo) [50,26] are indicated by green arrows. The role of molybdenum as a cofactor in nitrogen cycle reactions is indicated by dashed arrows. Differences in the relative rates of phosphorus [98] and nitrogen [93] cycling reactions are indicated by differences in the weight of arrows. DOC = dissolved organic carbon.

122 107]. Such negative feedbacks (Fig. 2) have been argued to lead to bi-stability on the path to full
 123 ocean oxygenation [108]. That is, full oxygenation ocean represents a biogeochemically stable
 124 state since it removes those factors that limit primary production, but while they are present those
 125 factors prevent oxygenation. It was therefore argued that transient large-scale perturbations in the
 126 redox state of the ocean due to global snowball Earth glaciations [82] were ultimately needed to
 127 trigger the transition to a fully oxygenated state [108].

128
 129 The framework outlined above can be expanded upon by taking an ecophysiological view of the
 130 genomic record across the Neoproterozoic-Phanerozoic boundary. Based off an analysis of the
 131 metabolic innovations seen in *Synechococcus* and *Prochlorococcus*, we recently argued that an
 132 additional negative feedback preventing ocean oxygenation was built into the machinery of
 133 photosynthesis itself [63] (Fig. 3). Oxygenic photosynthesis depends on substantial amounts of
 134 iron [109], but iron is highly insoluble under aerobic conditions, especially at the pH of ambient
 135 seawater [110,111]. Thus, as ocean oxygenation proceeded, iron would become increasingly
 136 scarce [86, 112], presenting a challenge not just to oxygenic photosynthesis (Fig. 3) but also to
 137 nitrogen fixation [113] and biological electron transfer more generally [114,115].

138
 139 This hypothesized feedback (Fig. 3) is fundamentally different than those involving phosphorus
 140 and nitrogen (Fig. 2), as it is strengthened rather than weakened as oxygenation proceeds. As a
 141 result, transient perturbations to the ocean redox state alone are ultimately insufficient to explain
 142 persistent oxygenation. An important clue to understanding how the biosphere nevertheless
 143 overcame this evolutionary bottleneck lies in the fact that in the extant oceans iron is not dissolved
 144 as free ions but instead is bound to a vast pool of dissolved organic carbon (Fig. 2) [116,117].
 145 While some iron is bound to special iron-scavenging siderophores, a large fraction is bound to
 146 more weakly-chelating compounds that are common metabolic intermediates or precursors of
 147 cellular building blocks, such as polysaccharides and simple carboxylic acids and/or alcohols
 148 [116,117,118,119]. This suggests that perhaps the evolution of cellular metabolism itself helped
 149 ancestral oxygenic photosynthesis overcome its inherently self-damping nature.

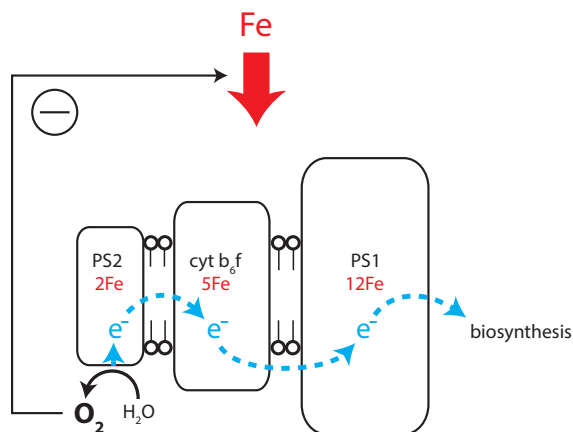


Fig. 3 Graphical representation of the hypothesis that ancestral cyanobacterial photosynthesis had a built-in negative feedback (black arrow highlighted by ‘-’ sign) that prevented its expansion into the deep open ocean. Relative sizes of electron transfer components reflect their cellular stoichiometry in cyanobacteria. Red lettering indicates the number of iron atoms that components require and red arrow reflects influx of iron that cells need to build photosynthetic machinery. Blue dashes arrows reflect the flow of electrons arising from water splitting. Abbreviations: PS2 = photosystem II, cyt b_6f = cytochrome b_6f , PS1 = photosystem I.

150

151

152

Metabolic evolution of marine picocyanobacteria

153 Marine picocyanobacteria provide an ideal model system for understanding the evolution of the

154 biogeochemical cycles as the ocean became oxygenated. Early evolution of this group took place

155 across the Neoproterozoic-Phanerozoic boundary [60,61], and its physiological, ecological and

156 genomic diversity has been characterized in detail [58,59,120]. We recently showed that as marine

157 picocyanobacteria colonized the oceans their metabolic core underwent a global remodeling [63]

158 (Fig. 4A). Remodeling is most extensive in *Prochlorococcus* and involves modifications to the

159 pigments and stoichiometry of the photosynthetic machinery [57,59,121-125] as well as to core

160 carbohydrate metabolism, wherein pathways were created for excreting organic carbon from the

161 cell [63] (Fig. 4A). The latter is inferred from a range of observations, including: 1) the truncation

162 of metabolic pathways that leave dead ends in the network (Fig. 4A), 2) genomic rearrangements

163 that place export transporters next to core metabolic enzymes, including those that catalyze the

164 final steps of truncated pathways [63], 3) synchronized gene expression of transporter-metabolic

165 enzyme pairs that follow the daily rhythms of solar energy input [126,63] and 4) experimental

166 studies showing excretion of glycolate [127], one of the identified dead end metabolites [Fig. 4A).

167 In addition to the low molecular weight carboxylic acids identified in these analyses (Fig. 4A),

168 experiments suggest that *Synechococcus* and *Prochlorococcus* also excrete significant amounts of

169 polysaccharides and other high molecular weight compounds [127-130].

170

171 Identifying the driving forces that underpin *Prochlorococcus*' metabolic innovations (Fig. 4A)

172 requires looking at the system at multiple levels. Based on the insolubility of iron under aerobic

173 conditions [110,111] it is tempting to conclude that cells evolved to excrete organic carbon to

174 enhance its bioavailability (Fig. 3). Similarly, the difficulty of culturing many oceanic microbes

175 without complex nutrient additions [131,132] suggests that interactions with sympatric

176 heterotrophs is part of what drove *Prochlorococcus*' metabolic evolution. However, both scenarios

177 involve extracellular sharing of resources between members of the community, and it is generally

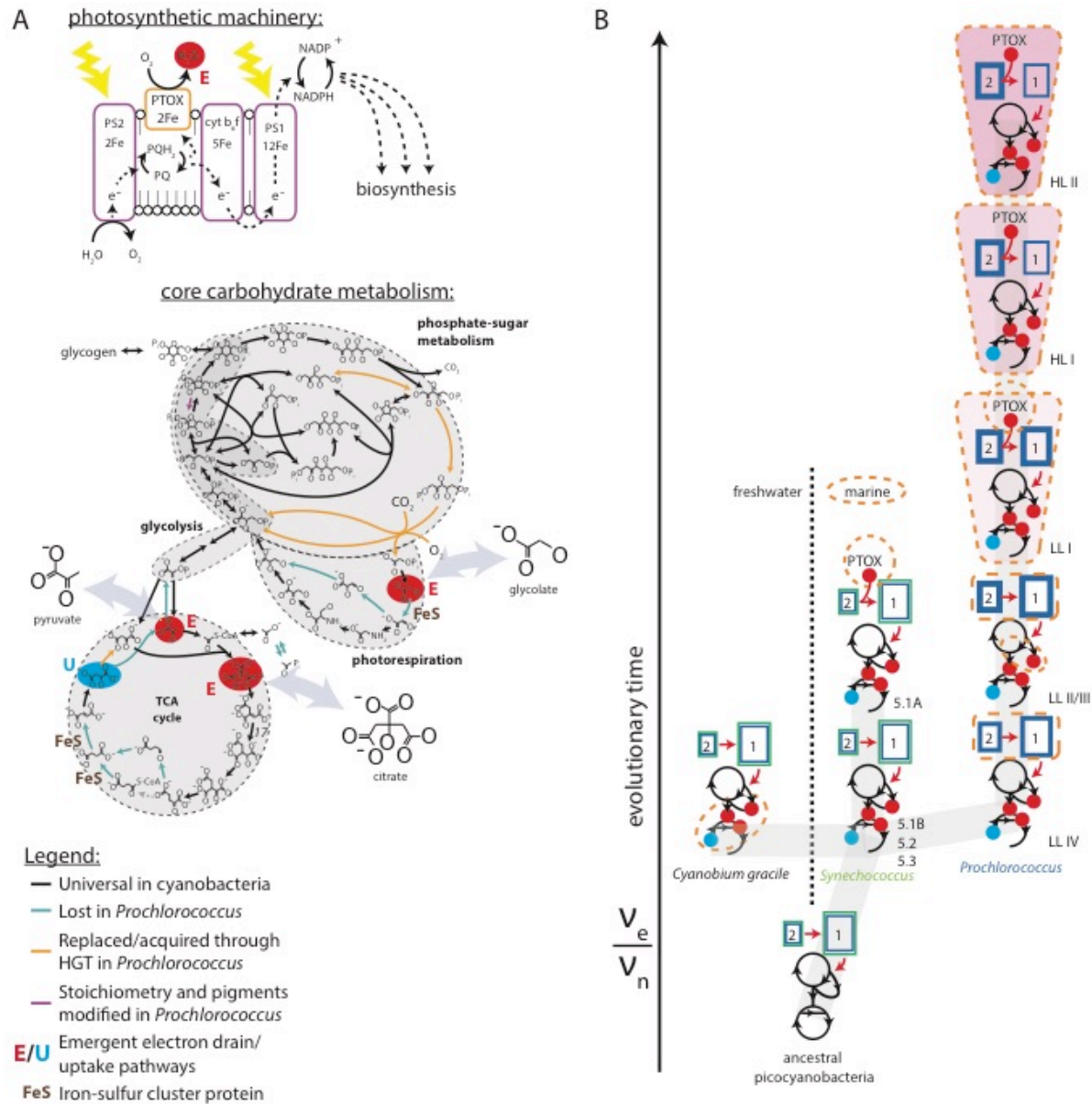


Fig. 4 Metabolic evolution of *Prochlorococcus*. **A)** Evolutionary changes in the metabolic core of *Prochlorococcus* relative to ancestral cyanobacteria, as indicated by colors in the inset [63]. Compounds identified as excretion pathways are highlighted with red dots and bi-directional grey arrows, while a compound identified as an uptake pathway is highlighted with a blue dot. **B)** Metabolic variants from panel A are drawn in simplified form along a gradient of an increasing electron-to-nutrient ratio, v_e/v_n . Red arrows indicate the flow of electrons and black arrows indicate the flow of carbon. The size of photosystem boxes reflects their cellular stoichiometry, their colors indicate major wavelengths of absorption and line thickness indicates absorption cross-section. Innovations are highlighted by dashed orange circles and those related to light damage protection/repair [137,138] are indicated by a darkening pink shade. Figure adapted from Figs. S1 & 4 from [63]. In the original tree in Ref [63] the phenotype of *Cyanobium gracile* was drawn as branching between ancestral picocyanobacteria and marine *Synechococcus*, but recent analyses suggest there were multiple incursions across the fresh water-marine boundary near the evolutionary roots of this group [139]. Abbreviations: LL = low-light adapted, HL = high-light adapted.

178 thought such social interactions can only evolve when physical collocation of cells across
179 generation ensures that resource benefits are transmitted directly from parents to offspring

180 [133,134]. In contrast, *Prochlorococcus* populations are made up of individual planktonic cells,
 181 and fluid dynamic calculations suggest that recently divided cells are separated by tens of meters
 182 within an hour and kilometers within a week [135], indicating they essentially never interact. Such
 183 well-mixed conditions are thought to lead to the “tragedy of the commons” [136], in which
 184 freeloading mutants that receive the benefits of shared resources but do not incur the costs of
 185 producing them take over the population and suppress sharing [133,134,136]. That selection
 186 nevertheless consistently favored the addition of pathways for excreting organic carbon in
 187 *Prochlorococcus* (Fig. 4A) suggests it must directly benefit individual cells, with any community-
 188 level benefits emerging as a by-product.

189
 190 Studies of aerobic heterotrophs that can facultatively switch between respiration and fermentation
 191 have identified benefits of excreting organic carbon that could be relevant to *Prochlorococcus*.
 192 Fermentation pathways that involve excretion of incompletely oxidized carbon are more
 193 thermodynamically downhill and can sustain higher rates of ATP production than respiration
 194 pathways that fully oxidize carbon to CO₂ [140-142]. This allows cells with plentiful supplies of
 195 organic carbon to increase their growth rates by switching to fermentation and redirecting protein
 196 biomass from ATP production to biosynthesis [143-145]. However, *Prochlorococcus* has a lower
 197 intrinsic growth rate compared to other cyanobacteria [57,146] and since excreting organic carbon
 198 occurs downstream of photosynthesis it would not appear to affect the protein biomass requirement
 199 of ATP production. Perhaps more relevant to *Prochlorococcus*, some aerobic heterotrophs also
 200 switch on fermentation pathways under nutrient-limited growth conditions, where it is thought to
 201 help maintain redox balance by providing an outlet for excess reducing power [147-150].
 202 However, many photosynthesizers can prevent redox imbalance by using ‘photoacclimation’ to
 203 decrease their harvesting of solar energy [153,154], and *Prochlorococcus* appears to have only a
 204 modest ability for photoacclimation [151,152]. This suggests there are other benefits to increasing
 205 the throughput and excretion of organic carbon than only responding to redox stress.

206
 207 A more complete view emerges when examining changes in *Prochlorococcus*’ metabolism in the
 208 context of its physiological, ecological and genomic diversity [58,59,120]. For example, in warm
 209 stable water columns *Prochlorococcus* differentiates by depth into a layered population structure,
 210 with recently diverging “high-light adapted” clades experiencing higher light levels near the
 211 surface and deeply branching “low-light adapted” clades experiencing lower light levels at the
 212 bottom of the euphotic zone [155-159]. Abovementioned changes to the photosystems [57,59,121-
 213 125] (Fig. 4A), which increase the absorption cross-section of cells [160,146], thus appear to
 214 reflect an evolutionary trend that increases the photosynthetic electron flux [63], defined as:

$$v_e = I\sigma_{PSII}\theta_{PSII}, \quad (1)$$

216
 217 where I is light intensity, σ_{PSII} is the total cellular absorption cross-section of photosystem II
 218 (where water-splitting leads to the generation of an electron flux) and θ_{PSII} is the quantum
 219 efficiency of absorption.

220
 221 An evolutionary increase in the photosynthetic electron flux further coincides with a general
 222 process of evolutionary ‘streamlining’ [161-163] that decreases the dependency of cells on
 223 phosphorus, nitrogen and iron, key limiting nutrients in the oceans [164]. For example,
 224 *Prochlorococcus* genomes have undergone reduction in size and guanosine-cytosine content (AT

225 base pairs require one fewer nitrogen atom than GC base pairs) [165], its proteins contain few
 226 nitrogen-rich amino acids [166], its membranes consist of glyco- and sulfolipids rather than
 227 phospholipids [167,168] and its modified metabolism (Fig. 4A) requires less iron [124,63]. Finally,
 228 *Prochlorococcus* has a lower growth rate than *Synechococcus*, which in turn has a lower growth
 229 rate than other cyanobacteria [57,146]. This suggests a decrease not just in the nutrient content of
 230 cells but in the uptake flux of nutrients [63], defined as:

$$231 \quad v_n = \mu Q_n, \quad (2)$$

232 where μ is the specific growth rate and Q_n is the cellular nutrient quota. Combined evidence thus
 233 suggests that the addition of pathways for excreting organic carbon – an extracellular sink for
 234 electrons – reflects a general increase in the total throughput of electrons, as defined by the
 235 electron-to-nutrient flux ratio of cells, v_e/v_n (Fig. 4B). Since the photosynthetic electron flux
 236 carries solar energy into metabolism, an increase in v_e/v_n suggests an increase in the metabolic
 237 rate (energy time⁻¹ mass⁻¹) of cells.

238 An important clue for why selection favor an increase in cellular metabolic rate comes from the
 239 extant population structure of *Prochlorococcus*. The most recently diverging, highest metabolic
 240 rate phenotypes (Fig. 4B) are the “high-light adapted” clades that live near the surface, where solar
 241 energy is abundant and nutrient concentrations are at their lowest [155-159]. This suggests there
 242 is a link between metabolic rate and nutrient acquisition [169,63], which can be elucidated by
 243 considering the free energy cost of the nutrient uptake reaction:

$$244 \quad \Delta G_r = \ln \left(\frac{[n]_I}{[n]_E} \right) + ZF\Delta\psi, \quad (3)$$

245 where Z is the unit charge of nutrient ions, F is the Faraday constant, $\Delta\psi$ is the membrane potential
 246 and subscripts I and E refer to internal and external nutrients, respectively. Eq. 1 shows that as
 247 environmental nutrient concentrations ($[n]_E$) decrease, stronger energetic driving is needed to
 248 facilitate nutrient uptake. For active transport (i.e. $n_E + ATP \rightleftharpoons n_I + ADP + P_i$), increasing the
 249 energetic driving is achieved by increasing the $[ATP]/[ADP \times P_i]$ ratio, which is observed under
 250 nutrient-limited growth conditions in bacterial, plant and algal cells alike [170-173].

251 A parsimonious interpretation of the evidence is thus that selection for an increased metabolic rate
 252 in *Prochlorococcus* has lowered the nutrient concentration at which cells can grow [63]. Still
 253 somewhat unclear are the molecular details of how an increased metabolic rate leads to an
 254 increased ATP/ADP ratio and why this requires organic carbon excretion. Since cellular
 255 metabolism continually consumes ATP, cells can only increase ATP/ADP if they can create a
 256 temporary imbalance between the rates of ATP production and consumption until a new steady
 257 state at higher potential is created. In fast-growing heterotrophic cells an increase in the ATP/ADP
 258 ratio is linked to an increase in the consumption of organic carbon and use of fermentative
 259 pathways leading to excretion of partially oxidized carbon [147-149,174,175]. Nutrient-limited
 260 growth conditions – which requires an increase in the ATP/ADP ratio (Eq. 1) – similarly lead to
 261 an increased throughput and excretion of organic carbon in both phytoplankton [175-179] and
 262 heterotrophs [147-150]. These observations suggest that cells use increased carbon and ATP
 263 supplies to drive pathways into saturation, keeping a larger fraction of enzymes occupied by all by

268 the limiting nutrient(s), thereby causing ATP production to outpace consumption and the
 269 ATP/ADP ratio to increase [63]. An increasing ATP/ADP ratio would in turn cause forward rates
 270 of ATP-consuming reactions to increase until ATP production and consumption are once again in
 271 balance. While in principle it would appear possible to drive pathways into saturation by
 272 decreasing their maximal rates (e.g. by lowering enzyme levels), possibly circumventing the need
 273 for excreting (excess) carbon, the pathways for assimilating carbon and limiting nutrients into
 274 biomass are intimately intertwined, making this a potentially counterproductive strategy.

275
 276 Thus, while further study is needed, combined evidence led us to conclude that evolutionary
 277 increases in cellular metabolic rate and organic carbon excretion (Fig. 4) reflect the same driving
 278 force and allow *Prochlorococcus* cells to grow at lower nutrient concentrations [63]. This
 279 hypothesis can be developed into a mathematical model in two steps, the first of which is to relate
 280 the nutrient uptake flux to the electron and carbon fluxes [63]:

$$v_n = \frac{Q_n}{Q_C} v_e (\#C/\#e)(1 - \beta), \quad (4)$$

282
 283 where Q_n/Q_C is the cellular stoichiometry of nutrient n and carbon, $\#C/\#e$ is the efficiency of
 284 carbon-fixation (i.e. the number of carbon that are fixed per electron obtained from water splitting),
 285 and β is the fraction ($0 < \beta < 1$) of the carbon flux that is excreted. The nutrient uptake flux can in
 286 turn be related to the free energy of the nutrient uptake reaction using reversible Michaelis-Menten
 287 kinetics [63]:

$$v_n = \frac{[n][E]k^+}{K_{M,n}} (1 - e^{\Delta_r G/RT}), \quad (5)$$

289
 290 where $[E]$ is the concentration of the uptake transporter enzyme, $K_{M,n}$ is its Michaelis constant,
 291 k^+ is the rate constant of the uptake reaction and the forward and backward reactions are related
 292 through $\Delta_r G = -RT \ln([n]_E K_{M,nE} K_{eq} / [n]_I K_{M,nI})$ [180]. Finally, equations 4 and 5 can be
 293 combined to relate relevant features of cells to the nutrient concentrations at which they can grow
 294 [63]:

$$[n] = \frac{K_{M,n} v_n}{[E]k^+(1 - e^{\Delta_r G/RT})} = \frac{K_{M,n} Q_n v_e (\#C/\#e)(1 - \beta)}{[E]k^+ Q_C (1 - e^{\Delta_r G/RT})}, \quad (6)$$

296
 297 Equation 6 immediately shows that selection for growth at lower nutrient concentrations favors a
 298 decrease in the nutrient uptake flux (v_n). However, as outlined above, resulting decreases in the
 299 minimal subsistence nutrient concentration $[n]$ are self-limiting because it increases the free
 300 energy cost of uptake $\Delta_r G$ (Eq. 3). As argued above, cells are able to compensate for this increased
 301 cost by driving metabolic pathways into saturation, thereby driving up the ATP/ADP ratio, and
 302 excreting the resulting excess carbon. By this logic Eq. 6 thus suggests that selection for growth at
 303 lower nutrient concentrations favors increasing v_e/v_n as well as the excretion of organic carbon,
 304 as observed in the evolution of *Prochlorococcus* (Fig. 4B).

305
 306

307
308
309
310
311
312
313
314
315
316
317
318
319

Evolutionary dynamics of *Prochlorococcus*

The reconstructed metabolic evolution (Fig. 4) and model of Eq. 6 provides a new perspective on the macroevolutionary diversification of *Prochlorococcus* and how it shaped the ocean ecosystem. It suggests the layered structure of extant *Prochlorococcus* populations [155-159] arose through a sequence of niche constructing adaptive radiations (Fig. 5). Each innovation that increased the harvesting of solar energy drew down nutrient levels at the surface, thereby restricting ancestral populations adapted to higher nutrient levels to greater depths, while driving up levels of dissolved organic carbon [63]. This in turn implies *Prochlorococcus* has an important role in shaping extant ocean chemistry, which is consistent with observations that its populations are densest in the tropical and sub-tropical surface oceans where nutrients are near-vanishing [157,159] and dissolved organic carbon levels are twice as high as in the rest of the oceans [182].

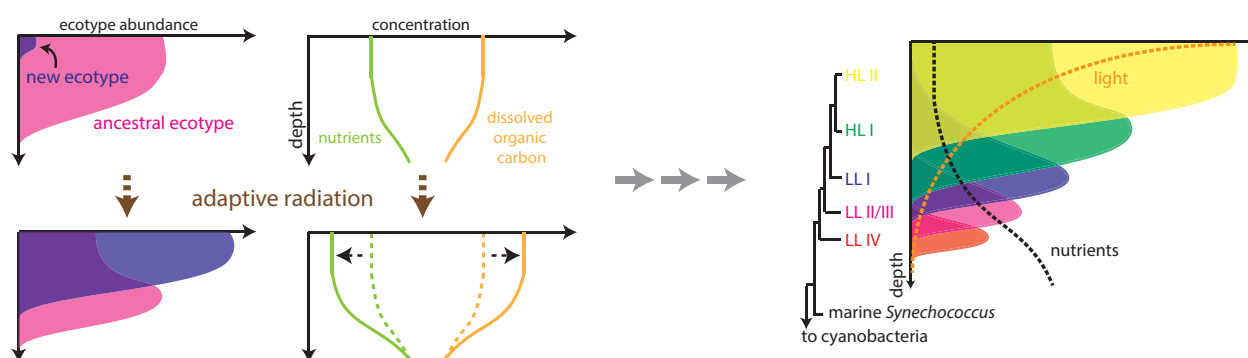


Fig. 5 Macroevolutionary dynamics leading to niche partitioning in *Prochlorococcus*. Panel on left shows the principles of niche constructing adaptive radiations. Innovations that increase cellular metabolic rate (Fig. 4) lead to the emergence of new populations (purple) that drive down nutrient levels (green curve) and increase dissolved organic carbon levels (orange curve). Ancestral populations (pink) are restricted to greater depth where nutrients remain elevated. A sequence of adaptive radiations leads to the extant population structure shown in panel on right. Populations are colored according to the labels on the consensus phylogeny shown next to the ecological panel. Adapted from Figs 1 & 4 from Ref [63].

320 The proposed dynamic (Fig. 5) is consistent with a recent study on the evolution of nitrate
321 assimilation in *Prochlorococcus* [183]. It was shown this trait is absent in basal *Prochlorococcus*
322 clades, even though its evolution is governed by vertical inheritance going back to before the
323 split between *Prochlorococcus* and *Synechococcus* [183]. Studies of seasonal ecological
324 dynamics in *Prochlorococcus* had previously shown that cells with the ability to assimilate
325 nitrate are selected for in summer months when light is intense and concentrations of all forms of
326 nitrogen are low [184]. This led to the conclusion that basal clades originally occupied more of
327 the water column before niche partitioning restricted them to the bottom of the water column
328 (Fig. 5) where retention of nitrate assimilation genes became unfavorable [183].

329

330

Evolution of biospheric productivity in the oceans

331

332 The reconstructed evolutionary dynamic of *Prochlorococcus* (Fig. 4B & 5, Eq. 6) provides general
333 insights into the evolution of the oceanic biosphere as a whole. Innovations increasing v_e/v_n reach
334 back to the last common ancestor of all marine picocyanobacteria (Fig. 4B), and since such
335 innovations allow cells to grow at lower nutrient concentrations (Eq. 6), it helps explain how this

336 group was able to colonize the open ocean in the face of nitrogen and/or phosphorus limitation
 337 (Fig. 2). Similarly, changes in the photosynthetic machinery and core metabolic pathways (Fig.
 338 4A) decrease the iron requirements of cells [63,124], helping explain how photosynthesis was able
 339 to begin extending its reach in the face of declining iron levels as the ocean became oxygenated
 340 (Fig. 3). In addition, the classes of organic carbon compounds excreted by marine
 341 picocyanobacteria (carboxylic acids, polysaccharides) are known to chelate iron and enhance its
 342 bioavailability [63,118,119]. Thus, the evolution of marine picocyanobacteria added a positive
 343 feedback (Fig. 6) that counteracted the negative feedbacks built-in to ancestral cyanobacterial
 344 photosynthesis (Fig. 3) and paved the way for ocean oxygenation.
 345

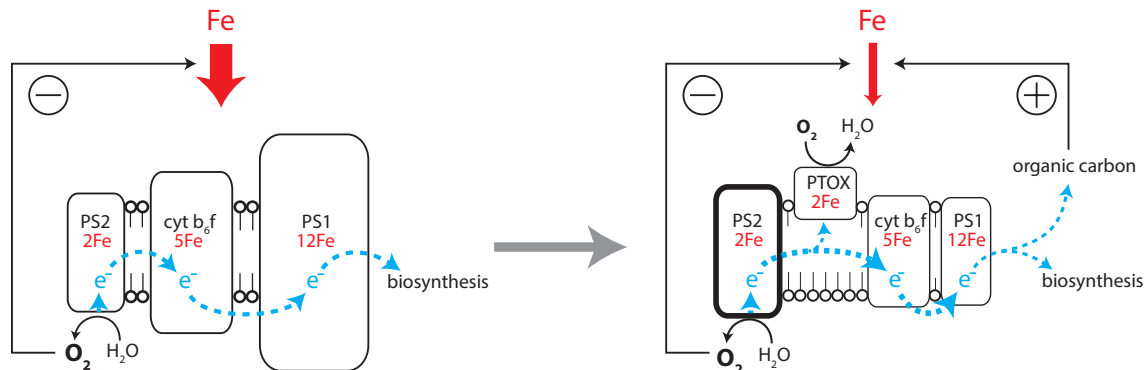


Fig. 6 Evolution of feedbacks involving iron in the machinery of photosynthesis. Left panel reflects photosynthetic machinery of ancestral cyanobacteria, right panel reflects photosynthetic machinery of *Prochlorococcus*. Relative size of electron transfer components reflects their cellular stoichiometry, line thickness reflects absorption cross-section. Relative thickness of red arrows reflects differences in the cellular iron fluxes (v_{Fe}) needed to build photosynthetic machinery. A positive feedback ('+' sign) emerging in the metabolic evolution of marine picocyanobacteria (Fig. 4) counteracts the negative feedback ('-' sign) built into the machinery of photosynthesis (Fig. 3). Dashed blue arrow reflects flow of electrons. Abbreviations: PTOX = plastoquinol terminal oxidase, others as in Fig. 3.

346 The identified positive feedback (Fig. 6) is linked to metabolic rate (Fig. 4), and so is strengthened
 347 with each innovation that enhances the harvesting of solar energy. The evolutionary process that
 348 produced such innovations in marine picocyanobacteria (Fig. 4) stretches out across the
 349 Neoproterozoic and Phanerozoic [60,61], which is relevant to discussion that ocean oxygenation
 350 played out over hundreds of millions of years [35,89-92]. Further, the innovations seen in marine
 351 picocyanobacteria (Fig. 4) are by no means unique to this group. Oceanic eukaryotic
 352 phytoplankton also have modified photosynthetic machineries that require less iron [185-187],
 353 modified membranes that require less phosphorus [167] and excrete large amounts of organic
 354 carbon under nutrient limitation [176-180]. This suggests that the reconstructed evolution of
 355 marine picocyanobacteria (Fig. 4) reflects general driving forces that allowed the oceanic
 356 biosphere as a whole to overcome the self-damping nature of ancestral cyanobacterial
 357 photosynthesis (Fig. 6).
 358

359 In principle, several additional positive biogeochemical feedbacks emerge from the positive
 360 feedback involving iron (Fig. 6). For example, the same classes of organic compounds (carboxylic
 361 acids, polysaccharides) released by marine picocyanobacteria are produced in terrestrial
 362 ecosystems and are known to enhance the weathering of rock minerals, releasing the iron and
 363 phosphorus they contain [188,189]. In the open ocean, rock minerals in wind-blown desert dust

364 are the major source of iron [190], as well as a source of phosphorus [191,192]. Thus, the evolution
365 of marine picocyanobacteria not only enhanced the bioavailability of iron as the ocean became
366 oxygenated, but potentially also increased the supply of available iron and phosphorus into the
367 oceans [63]. Such a link between the cycles of iron and phosphorus is consistent with observations
368 that some oceanic heterotrophs release iron-chelating compounds when they are phosphorus-
369 limited, presumably to dissolve minerals containing both iron and phosphorus [193]. In addition,
370 while photosynthetically-produced organic carbon enhanced the bioavailability of iron in
371 oxygenated environments (Fig. 6), overall iron levels still decreased significantly relative to those
372 in the previously anoxic oceans [112]. This led to a decrease in the scavenging of phosphorus (Fig.
373 2) and a concomitant increase in its bioavailability [94-97]. Ocean oxygenation would have also
374 lessened phosphorus limitation by increasing the supply of electron acceptors for the
375 remineralization of organic phosphorus [98] (Fig. 2).

376
377 Further, the drawdown of nitrogen near the surface (Fig. 5) and an enhancement in the
378 bioavailability of iron (Fig. 6) leads to conditions that generally promotes nitrogen-fixation [194-
379 196]. Ocean oxygenation would have moreover lifted any molybdenum-limitation by suppressing
380 euxinia (Fig. 2), creating generally prime conditions for the expansion of oceanic nitrogen-fixation
381 [50,26] and lessened nitrogen-limitation by decreasing the rate of denitrification relative to
382 nitrification [93] (Fig. 2). These scenarios are consistent with molecular clocks that estimate
383 Neoproterozoic origins of both planktonic marine nitrogen-fixers [60] and ammonia-oxidizing
384 marine Thaumarcheota [197,198], both of which indicate an increasing influx and cycling of fixed
385 nitrogen in the oceans. The geologic record leads to a similar conclusion, as sedimentary nitrogen
386 isotopes display shifts toward modern ocean values in the Neoproterozoic, indicating the onset of
387 a stable oceanic nitrate pool [101-107].

388 **Convergent biogeochemical evolution in the oceans and on the continents**

389
390
391 There are a wide range of parallels between the rise of marine picocyanobacteria and the rise of
392 land plants. Key observations at the level of cellular metabolism come from analyses of the highly
393 abundant oceanic alphaproteobacteria SAR11 [162,199], which like marine picocyanobacteria is
394 estimated to have emerged during the Neoproterozoic [200]. Reconstructions suggest the
395 metabolic core of SAR11 underwent a global remodeling that was complementary to that of
396 *Prochlorococcus* (Fig. 4A), resulting in compatible pathways for the exchange of organic carbon
397 between the two groups (Fig. 7, top panel) [63]. This is consistent with previous experiments that
398 showed that SAR11 requires several of the compounds identified as excretion pathways in
399 *Prochlorococcus* (Fig. 4A) [201,132]. The pathways involved in these exchanges are highly
400 similar to those mediating metabolic interactions between chloroplasts and mitochondria in green
401 plant cells. Intermediates of lower glycolysis and photorespiration mediate the flow of electrons
402 and carbon from the photosynthetic to the heterotrophic components in both plant cells and in
403 oceanic microbial ecosystems, while intermediates of the citric acid cycle mediate the flow of
404 electrons and carbon in the opposite direction (Fig. 4A) [63].

405
406 Convergence in the metabolic evolution of the two systems extends from core pathways to their
407 energy metabolism (Fig. 7, top panel). *Prochlorococcus* uses chlorophyll a and b instead of
408 phycobilisomes [57] and has a PSII/PSI ratio that is significantly higher than other cyanobacteria
409 [123,202,203], making its photosynthetic machinery rather more like that of green chloroplasts

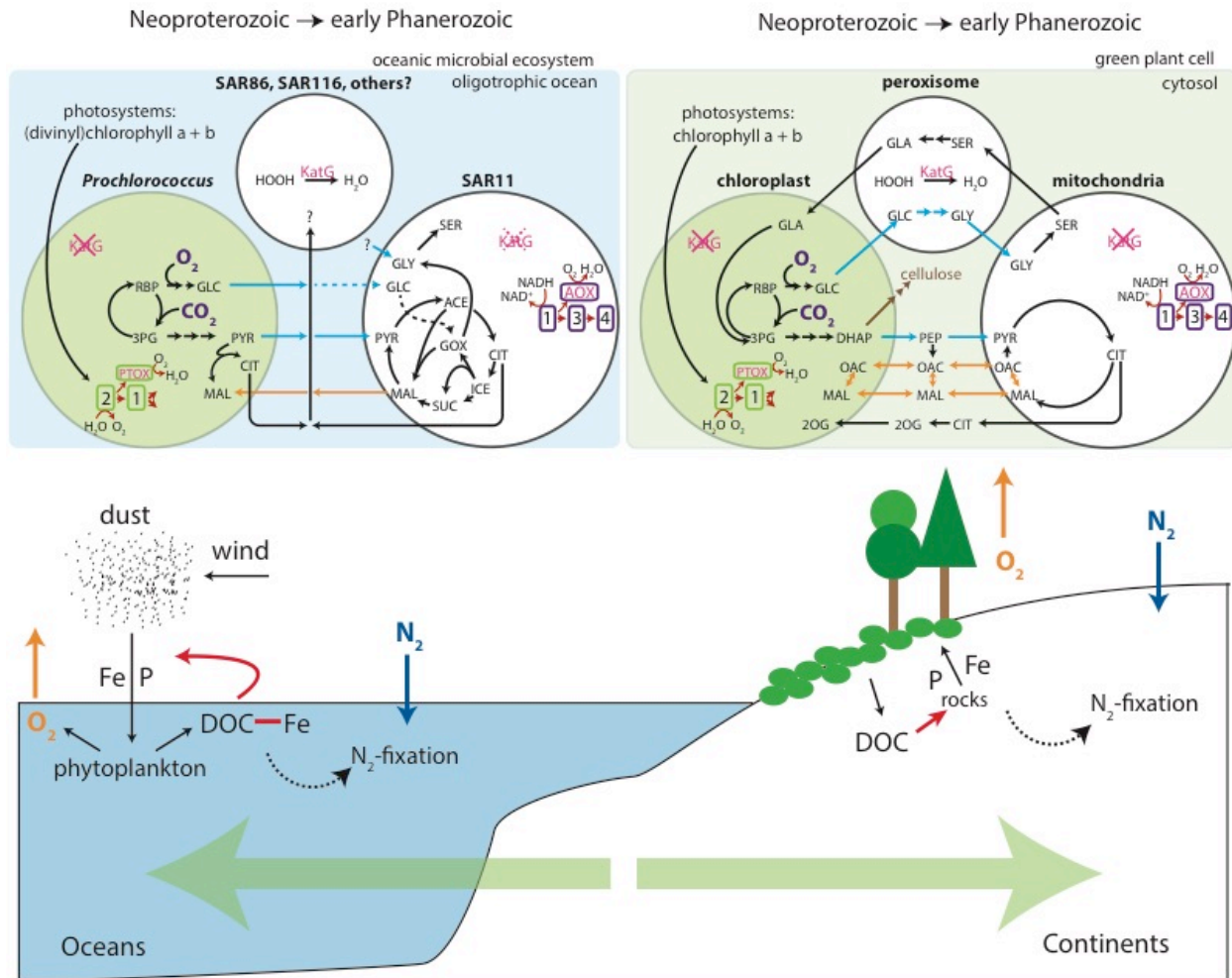


Fig. 7 Convergent biogeochemical evolution of green eukaryotic photosynthesis in the oceans and on the continents. Top panel: Similarities between the photosystems, electron transport chains and core carbohydrate metabolic pathways of oceanic microbial ecosystems and green plant cells. Metabolic reactions are shown in simplified form not accounting for stoichiometry. Blue arrows indicate flow of electrons and carbon from autotrophic to heterotrophic components, while orange arrows indicate flow of electrons and carbon in opposite direction. Bottom panel: Geochemical feedbacks driven by the evolution of eukaryotic photosynthesis on land and in the sea. Big green arrows indicate ecological expansion of green eukaryotic photosynthesis (panel A) away from continental boundaries. Red arrows reflect positive weathering feedbacks of photosynthetically produced organic carbon. Dashed arrows reflect the stimulation of nitrogen-fixation and dark blue arrows reflect increasing influx of nitrogen from the atmosphere into the oceanic/terrestrial biogeochemical cycles and. Orange arrows represent the increasing oxygen flux into the atmosphere due to increasing biospheric productivity. Top panel adapted from Fig. 5 of Ref [63] Abbreviations: RBP = ribose bisphosphate, GLC = glycolate, PYR = pyruvate, CIT = citrate, MAL = malate, GLY = glycine, SER = serine, ACE = acetyl-CoA, GOX = glyoxylate, SUC = succinate, ICE = isocitrate, GLA = glycerate, OAC = oxaloacetate, 2OG = 2-oxoglutarate, AOX = alternative oxidase, PTOX = plastoquino terminal oxidase, KatG = catalase

410 than other cyanobacteria [63]. The electron transport chains of the two systems further contain
 411 similar bypasses. The electron transport chains of *Prochlorococcus* and chloroplasts both contain
 412 plastoquinol terminal oxidase (PTOX), which creates a water-water cycle by redirecting electron
 413 flux immediately following photosystem II [124,204]. The electron transport chains of SAR11 and
 414 mitochondria in turn both contain alternative oxidase, which again creates a short cut in the
 415 reduction of oxygen to water by redirecting electrons immediately following complex I [204,205].

416 Finally, *Prochlorococcus* and some clades of SAR11 have lost catalase and the ability to detoxify
417 peroxide (HOOH), a by-product of photosynthesis, and depend on other sympatric microbes for
418 this function [206,207], just as chloroplasts and mitochondria depend on the peroxisome for this
419 function [205].

420
421 Similarities between oceanic microbial ecosystems and land plants also include the timing and
422 biogeochemical impact of their emergence on the Earth system (Fig. 7, bottom panel). The
423 expansion of plants onto the continents dates to the early Phanerozoic [45], while their
424 evolutionary roots lie in the Neoproterozoic [52,208-211], similar to the timeframes over which
425 ancestral marine picocyanobacteria diversified into *Synechococcus* and *Prochlorococcus* [60,61].
426 In addition, under nutrient limitation plants excrete organic carbon from their roots, dissolving
427 rocks minerals and making the iron and phosphorus within them available [212,213]. The resulting
428 conditions promote nitrogen-fixation [194-196], and various plants have evolved symbioses with
429 nitrogen-fixing bacteria in their rhizosphere [195,214], increasing the supply of fixed nitrogen into
430 the terrestrial biosphere [214]. This is consistent with molecular clocks estimating a
431 Neoproterozoic rise of ammonia-oxidizing Thaumarcheota in terrestrial soils [197,198],
432 paralleling their aforementioned Neoproterozoic rise in the oceans [197,198]. These observations
433 have led to the arguments that the rise of land plants enhanced continental weathering and organic
434 carbon burial as the productivity of the terrestrial biosphere increased, driving an increase in
435 atmospheric oxygen [216,217] (Fig. 7, bottom panel). The proposal outlined above (Fig. 6 and
436 surrounding discussion) extends those arguments to the water column and highlights the
437 convergent biogeochemical evolution of eukaryotic photosynthesis on land and in the sea (Fig. 7)
438 [63].

439 440 **Outlook: biospheric self-amplification, plate tectonics and Earth oxygenation**

441
442 Cellular metabolism provides a unique lens into Earth history [218]. Looking through this lens in
443 marine picocyanobacteria leads to a general framework in which ecosystems follow self-
444 amplifying evolutionary trajectories (Fig. 8) [63]. This holds for particular groups, for example
445 in the niche partitioning of *Prochlorococcus* (Fig. 5), as well as for the biosphere as a whole. As
446 cells acquire innovations that allow them to obtain ever-sparsier nutrients (Fig. 4, Eq. 6), more
447 nutrients are driven from the environment into the living state, increasing total ecosystem
448 biomass (Fig. 5 & 8). This in turn promotes the mobilization of nutrients at larger scales, for
449 example through enhanced weathering of rocks in the case of iron and phosphorus, or by creating
450 opportunities for nitrogen-fixers in the case of nitrogen (Fig. 7).

451
452 At the largest scale, the two major stages of biospheric expansion and Earth oxygenation are
453 linked to the bioenergetic innovations of cyanobacterial and eukaryotic photosynthesis [63]. A
454 combination of feedbacks (Figs. 2 & 3) prevented cyanobacterial photosynthesis from expanding
455 away from shallow aquatic environments near continental boundaries where weathering inputs
456 made nutrients relatively more easily accessible than in the open ocean or on the continents. The
457 increasing cellular energy flux and associated production of organic carbon of eukaryotic
458 photosynthesis, which from a metabolic perspective includes marine picocyanobacteria (Fig. 7),
459 helped the biosphere push through these negative feedbacks and expand into the open ocean and
460 onto the continents where nutrients were inherently harder to come by as oxygenation proceeded
461 (Figs. 6 & 7). This scenario is consistent with phylogenomic analyses suggesting freshwater
462 origins for both cyanobacteria and photosynthetic eukaryotes [219,220] and molecular biomarker

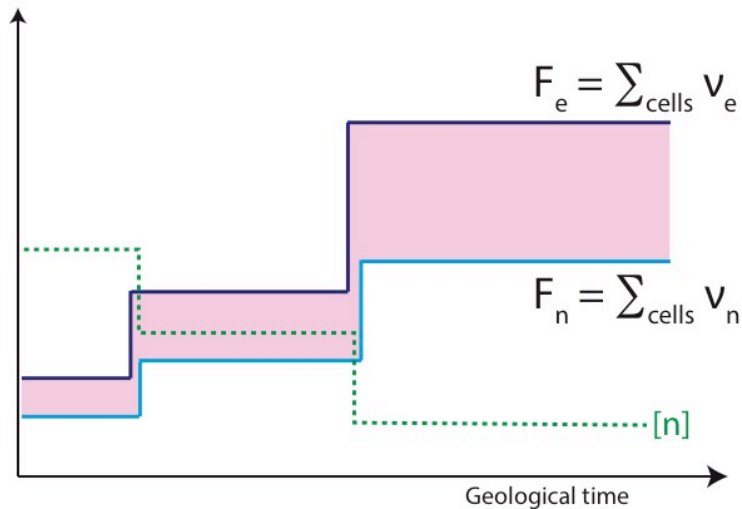


Fig. 8. Evolution of ecosystem-level fluxes of electron and nutrients ($F_{e,n}$) and environmental nutrient concentrations over geologic time. Innovations that increase metabolic rate (through increases in the electron-to-nutrient flux ratio, v_e/v_n) increase total ecosystem biomass by making more nutrients bioavailable and driving them into the living state (Fig. 5). At larger scales this promotes the influx of nutrients into the ecosystem from surrounding environments, through enhanced nitrogen-fixation and/or weathering feedbacks (Fig. 7). Ecosystem-level electron and nutrient fluxes $F_{e,n}$ are the sum (\sum_{cells}) of cellular nutrient and electron fluxes that make up the ecosystem.

463 studies indicating a major expansion of eukaryotic green algae in the marine realm in the late
 464 Neoproterozoic [52]. The faster sinking of larger organisms and/or their fecal pellets [38-41]
 465 likely still acted as a positive feedback promoting ocean oxygenation in the Neoproterozoic and
 466 Phanerozoic (Fig. 1), but this feedback was driven from the bottom up as more food became
 467 available to higher trophic levels (Fig. 5 & 8) [52].
 468

469 In addition to being linked to major increases in biospheric productivity, the periods of Earth
 470 history around the Great and Neoproterozoic Oxidation Events share a number of other
 471 similarities. As with the Neoproterozoic-Phanerozoic boundary, sediments near the Archean-
 472 Proterozoic boundary indicate a turbulent climate, with major carbon cycle perturbations
 473 [33,221,222] and global glaciation events [223-227]. And, while the evolution of plate tectonics is
 474 vigorously debated, a range of geological and geochemical evidence suggests its initiation in the
 475 Neoproterozoic [15,16,72,228-232] and a shift toward deeper subduction of colder and thicker crust
 476 in the Neoproterozoic [66,68-71,73,74,77]. Both epochs thus appear to mark major transitions in
 477 the dynamics of the whole Earth system.
 478

479 Major questions remain regarding the relative timing of the major bioenergetic innovations of
 480 photosynthesis and increases in atmospheric oxygen, as well as the time courses of the latter.
 481 Molecular clock estimates of when cyanobacteria or photosynthetic eukaryotes arose often
 482 disagree significantly with one another, to a large degree because of differences in the external
 483 date constraints (e.g. from fossils, biomarkers or other geochemical proxies) that are imposed on
 484 the calculations [209-211,233-238]. Nevertheless, a range of evidence suggests that the roots of
 485 cyanobacteria and the initiation of atmospheric oxygenation pre-date the Great Oxidation Event
 486 by several hundred million years [233,236,238-246]. Similarly, paleontological evidence and
 487 molecular clock estimates generally agree the roots of eukaryotic photosynthesis pre-date the
 488 Neoproterozoic Oxidation Event by at least several hundred million years [209-211,234,237]. If

489 photosynthetic innovations are ultimately responsible for both stages of oxygenation, what led to
490 these long delays?

491
492 Perhaps changes in the nature of plate tectonics are part of the explanation. A significant
493 Neoproterozoic increase in the exposed continental surface area has been linked to both the
494 initiation of plate tectonics [15,16,72,228-232] and to an associated increased influx of water into
495 the mantle [16,247-249]. Thus, if early cyanobacterial photosynthesis were restricted to
496 freshwater habitats [219] and continental boundaries (Fig. 7) [63], then growth of the size of
497 exposed continents and continental boundaries would drive an ecological expansion of
498 cyanobacteria over hundreds of millions of years. Moreover, the emergence of what we today
499 recognize as cyanobacterial photosynthesis involved an elaborate set of innovations,
500 encompassing core pathways, cofactors, photosystems, as well as damage protection
501 mechanisms needed to adapt to a changing environment [3,250-255] and these were likely
502 acquired over time rather than all at once. Oxygen accumulation further led to the eventual
503 emergence of an ozone layer [22], which filtered out damaging UV radiation and allowed
504 cyanobacteria to continue their expansion [256]. Thus, the size of habitats available to
505 cyanobacteria and their ability to fill those habitats likely increased in tandem during the rise of
506 continents. Indeed, it has been argued that the evolution of photosynthesis directly influenced the
507 initiation of plate tectonics by increasing the chemical weathering of continents, thereby
508 changing their composition and increasing the influx of water and other volatiles into the mantle
509 [257-262].

510
511 A generally similar scenario may have played out in the Neoproterozoic. It has been argued the
512 Neoproterozoic marked another increase in continental exposure as cold deep subduction was
513 initiated [68-71,73,74], the influx of water into the mantle increased [70,262], and crustal
514 buoyancy increased [263]. This is consistent with observations of a great ‘unconformity’ in
515 Neoproterozoic sediments that indicates a significant drop in seawater levels and enhanced
516 weathering of more exposed continents [66,75-77,262]. On the biological side, the reconstructed
517 evolution of marine picocyanobacteria (Fig. 4) highlights how the diversification and ecological
518 expansion of eukaryotic photosynthesis involved the sequential acquisition of a range of
519 innovations [63] over the course of hundreds of millions of years [60,61]. Finally, as mentioned
520 above, plants are known to chemically weather rocks [212,213], which led to the argument that
521 the rise of land plants played a central role in the enhanced large-scale weathering of continents
522 from the early Phanerozoic onward [264-267]. Evidence thus again points to a pattern of intimate
523 co-evolution of photosynthesis and dynamics of Earth’s crust and mantle over hundreds of millions
524 of years during the Neoproterozoic and early Phanerozoic.

525
526 The apparent similarities of Neoproterozoic and Neoproterozoic transitions in whole-Earth dynamics
527 raises the possibility of similar positive feedbacks operating in both epochs. As the weatherability
528 of continents increased in stages corresponding to their emergence, the actualized weathering rates
529 increased in stages corresponding to biospheric self-amplification, with these mechanisms
530 reinforcing each other. The weathering of rocks supplied the biosphere with key nutrients that
531 fueled its expansion [Fig. 7 & 8), while subduction of volatile-bearing sediments produced through
532 weathering helped fuel the rise of continents. The operation of such feedbacks is consistent with
533 statistical analyses of the large-scale sediment record, which identified significant long-term
534 increases in weathering and sedimentation rates in both the Neoproterozoic and Neoproterozoic

535 [75,268,269]. If transitions in biogeochemical cycling at the surface and in the crust and mantle
536 are fundamentally intertwined through weathering and subduction [257-262], then the long delays
537 between photosynthetic innovations and rises in atmospheric oxygen may simply reflect the
538 significantly greater inertia and longer timescales of change in solid Earth dynamics relative to
539 changes in the dynamics of the biosphere, oceans and atmosphere.

540
541 A fundamental link between biospheric productivity and weathering and sedimentation rates is
542 also consistent with the large-scale record of sedimentary carbon. Isotopic patterns in this record
543 indicate that the fraction of total carbon buried in sediments derived from organic carbon and
544 inorganic carbonates is stable at a ratio of around ~20:80 throughout most of Earth history,
545 although large transient divergences from this ratio are seen around both the Great and
546 Neoproterozoic Oxidation Events [4,5]. The sediment record itself thus indicates that any major
547 increases in the steady state burial of organic carbon must have been coupled to similar increases
548 in the steady state burial of carbonates.

549
550 If increases in biospheric productivity increased weathering and sedimentation rates it was also
551 help answer a conundrum regarding the relationship between the mechanisms of organic carbon
552 burial and atmospheric oxygenation. The fraction of organic carbon that is ultimately buried after
553 deposition in sediments is inversely proportional to the “oxygen exposure time”, a measure that is
554 the product of the overall sedimentation rate and how deeply oxygen penetrates into sediments,
555 which in turn depends on the oxygen concentration of bottom waters [270]. As a consequence,
556 Earth oxygenation effectively stymies itself by decreasing the fractional burial of sedimentary
557 carbon, unless increases in oxygen levels are coupled to increases in sedimentation rates and/or
558 changes in the composition of sediments that make them harder for oxygen to penetrate [4].
559 Evidence for the latter in the late Neoproterozoic and early Phanerozoic comes from analyses that
560 suggest biologically-driven increases in the production of fine-grained clays and muds [42,43,271-
561 273]. Thus, increases in the overall production sedimentation rates and in the production of less-
562 penetrable sediments worked together to counteract the negative effect of oxygenation on carbon
563 burial, allowing oxygen to rise.

564
565 The general framework outlined here leaves many questions unanswered. Why do major
566 transitions in Earth’s biogeochemical dynamics during the Neoproterozoic and Neoproterozoic
567 happen when they do? Is it simply that the gradual cooling of the crust and mantle eventually
568 passes through tipping points that cause changes in plate tectonics that trigger biospheric changes
569 and the emergence of self-reinforcing feedbacks? Or do biological innovations play a more
570 significant role, effectively speeding up the cooling of the solid Earth and pushing it toward tipping
571 points? At finer temporal scales, what is the ordering and causal relationship of geological and
572 biological changes that make up large-scale transitions? Do biological innovations ultimately drive
573 climate perturbations through carbon cycle perturbations, or do geologically-driven climate
574 changes trigger biological innovations, or is it both? Regardless of the exact details, the evidence
575 of broad parallels between the transitions in the physical, chemical and biological dynamics of
576 Earth during the Neoproterozoic and Neoproterozoic calls for general frameworks that treat these
577 periods together.

578
579
580

581 **Acknowledgements**

582
583 I thank Penny Chisholm and Mick Follows for generous support, encouragement and
584 collaboration during the development of the ideas outlined here. I further thank Kristin
585 Bergmann, Paul Berube, Daniel Rothman, Patricia Sanchez-Barracaldo, Paul Falkowski, Forrest
586 Horton, John Raven, Ron Milo, Peter Cawood, Eric Smith and Yuichiro Ueno for useful
587 feedback, discussions and suggestions of key references. This work was supported by a Simons
588 Foundation Fellowship of the Life Sciences Research Foundation (to R.B), by the Simons
589 Collaboration on Ocean Processes and Ecology, Award 329108 (to S.W. Chisholm and M.J.
590 Follows) and by Simons Foundation Life Sciences Project Awards 337262 and
591 509034SCFY17 (to S.W. Chisholm).

592
593 **References**

- 594
595 [1] Holland, H.D., 1984. *The chemical evolution of the atmosphere and oceans*. Princeton University Press.
596 [2] Hayes, J.M. and Waldbauer, J.R., 2006. The carbon cycle and associated redox processes through
597 time. *Philosophical Transactions of the Royal Society of London B: Biological Sciences*, 361(1470), pp.931-
598 950.
599 [3] Falkowski, P.G. and Raven, J.A., 2007. *Aquatic photosynthesis*, 2nd ED. Princeton University Press.
600 [4] Rothman, D., 2015. Earth's carbon cycle: a mathematical perspective. *Bulletin of the American Mathematical*
601 *Society*, 52(1), pp.47-64.
602 [5] Krissansen-Totton, J., Buick, R. and Catling, D.C., 2015. A statistical analysis of the carbon isotope record from
603 the Archean to Phanerozoic and implications for the rise of oxygen. *American Journal of Science*, 315(4),
604 pp.275-316.
605 [6] Ganino, C. and Arndt, N.T., 2009. Climate changes caused by degassing of sediments during the emplacement of
606 large igneous provinces. *Geology*, 37(4), pp.323-326.
607 [7] Stachel, T., Brey, G.P. and Harris, J.W., 2005. Inclusions in sublithospheric diamonds: glimpses of deep
608 Earth. *Elements*, 1(2), pp.73-78.
609 [8] Walter, M.J., Kohn, S.C., Araujo, D., Bulanova, G.P., Smith, C.B., Gaillou, E., Wang, J., Steele, A. and Shirey,
610 S.B., 2011. Deep mantle cycling of oceanic crust: evidence from diamonds and their mineral
611 inclusions. *Science*, p.1209300.
612 [9] Sverjensky, D.A., Stagno, V. and Huang, F., 2014. Important role for organic carbon in subduction-zone fluids in
613 the deep carbon cycle. *Nature Geoscience*, 7(12), p.909.
614 [10] Buseck, P.R. and Beyssac, O., 2014. From organic matter to graphite: Graphitization. *Elements*, 10(6), pp.421-
615 426.
616 [11] Galvez, M.E., Connolly, J.A. and Manning, C.E., 2016. Implications for metal and volatile cycles from the pH
617 of subduction zone fluids. *Nature*, 539(7629), p.420.
618 [12] Duncan, M.S. and Dasgupta, R., 2017. Rise of Earth's atmospheric oxygen controlled by efficient subduction of
619 organic carbon. *Nature Geoscience*, 10(5), p.387.
620 [13] Kasting, J.F., Egger, D.H. and Raeburn, S.P., 1993. Mantle redox evolution and the oxidation state of the
621 Archean atmosphere. *The Journal of geology*, 101(2), pp.245-257.
622 [14] Holland, H.D., 2002. Volcanic gases, black smokers, and the Great Oxidation Event. *Geochimica et*
623 *Cosmochimica Acta*, 66(21), pp.3811-3826.
624 [15] Kump, L.R. and Barley, M.E., 2007. Increased subaerial volcanism and the rise of atmospheric oxygen 2.5
625 billion years ago. *Nature*, 448(7157), p.1033.
626 [16] Gaillard, F., Scailliet, B. and Arndt, N.T., 2011. Atmospheric oxygenation caused by a change in volcanic
627 degassing pressure. *Nature*, 478(7368), p.229.
628 [17] Lee, C.T.A., Yeung, L.Y., McKenzie, N.R., Yokoyama, Y., Ozaki, K. and Lenardic, A., 2016. Two-step rise of
629 atmospheric oxygen linked to the growth of continents. *Nature Geoscience*, 9(6), p.417.
630 [18] Smit, M.A. and Mezger, K., 2017. Earth's early O₂ cycle suppressed by primitive continents. *Nature*
631 *geoscience*, 10(10), p.788.
632 [19] Cloud, P.E., 1968. Atmospheric and hydrospheric evolution on the primitive Earth. *Science*, 160(3829), pp.729-
633 736.

- 634 [20] Walker, J.C., 1977. Evolution of the Atmosphere. *New York: Macmillan, and London: Collier Macmillan,*
635 *1977.*
- 636 [21] Kasting, J.F., 1987. Theoretical constraints on oxygen and carbon dioxide concentrations in the Precambrian
637 atmosphere. *Precambrian research*, 34(3-4), pp.205-229.
- 638 [22] Farquhar, J., Bao, H. and Thiemens, M., 2000. Atmospheric influence of Earth's earliest sulfur
639 cycle. *Science*, 289(5480), pp.756-758.
- 640 [23] Bekker, A., Holland, H.D., Wang, P.L., Rumble Iii, D., Stein, H.J., Hannah, J.L., Coetzee, L.L. and Beukes,
641 N.J., 2004. Dating the rise of atmospheric oxygen. *Nature*, 427(6970), p.117.
- 642 [24] Luo, G., Ono, S., Beukes, N.J., Wang, D.T., Xie, S. and Summons, R.E., 2016. Rapid oxygenation of Earth's
643 atmosphere 2.33 billion years ago. *Science Advances*, 2(5), p.e1600134.
- 644 [25] Blättler, C.L., Claire, M.W., Prave, A.R., Kirsimäe, K., Higgins, J.A., Medvedev, P.V., Romashkin, A.E.,
645 Rychanchik, D.V., Zerkle, A.L., Paiste, K. and Kreitsmann, T., 2018. Two-billion-year-old evaporites capture
646 Earth's great oxidation. *Science*, 360(6386), pp.320-323.
- 647 [26] Reinhard, C.T., Planavsky, N.J., Robbins, L.J., Partin, C.A., Gill, B.C., Lalonde, S.V., Bekker, A., Konhauser,
648 K.O. and Lyons, T.W., 2013. Proterozoic ocean redox and biogeochemical stasis. *Proceedings of the National*
649 *Academy of Sciences*, p.201208622.
- 650 [27] Cawood, P.A. and Hawkesworth, C.J., 2014. Earth's middle age. *Geology*, 42(6), pp.503-506.
- 651 [28] Planavsky, N.J., Cole, D.B., Isson, T.T., Reinhard, C.T., Crockford, P.W., Sheldon, N.D. and Lyons, T.W.,
652 2018. A case for low atmospheric oxygen levels during Earth's middle history. *Emerging Topics in Life*
653 *Sciences*, p.ETLS20170161.
- 654 [29] Cloud Jr, P.E., 1948. Some problems and patterns of evolution exemplified by fossil
655 invertebrates. *Evolution*, 2(4), pp.322-350.
- 656 [30] Berkner, L.V. and Marshall, L.C., 1965. History of major atmospheric components. *Proceedings of the*
657 *National Academy of Sciences*, 53 (6) 1215-1226
- 658 [31] Runnegar, B., 1991. Precambrian oxygen levels estimated from the biochemistry and physiology of early
659 eukaryotes. *Palaeogeography, Palaeoclimatology, Palaeoecology*, 97(1-2), pp.97-111.
- 660 [32] Derry, L.A., Kaufman, A.J. and Jacobsen, S.B., 1992. Sedimentary cycling and environmental change in the
661 Late Proterozoic: evidence from stable and radiogenic isotopes. *Geochimica et Cosmochimica Acta*, 56(3),
662 pp.1317-1329.
- 663 [33] Des Marais, D.J., Strauss, H., Summons, R.E. and Hayes, J.M., 1992. Carbon isotope evidence for the stepwise
664 oxidation of the Proterozoic environment. *Nature*, 359(6396), p.605.
- 665 [34] Canfield, D.E. and Teske, A., 1996. Late Proterozoic rise in atmospheric oxygen concentration inferred from
666 phylogenetic and sulphur-isotope studies. *Nature*, 382(6587), p.127.
- 667 [35] Fike, D.A., Grotzinger, J.P., Pratt, L.M. and Summons, R.E., 2006. Oxidation of the Ediacaran
668 ocean. *nature*, 444(7120), p.744.
- 669 [36] Erwin, D.H., Laflamme, M., Tweedt, S.M., Sperling, E.A., Pisani, D. and Peterson, K.J., 2011. The Cambrian
670 conundrum: early divergence and later ecological success in the early history of animals. *science*, 334(6059),
671 pp.1091-1097.
- 672 [37] Och, L.M. and Shields-Zhou, G.A., 2012. The Neoproterozoic oxygenation event: Environmental perturbations
673 and biogeochemical cycling. *Earth-Science Reviews*, 110(1-4), pp.26-57.
- 674 [38] Knoll, A.H., Hayes, J.M., Kaufman, A.J., Swett, K. and Lambert, I.B., 1986. Secular variation in carbon isotope
675 ratios from Upper Proterozoic successions of Svalbard and East Greenland. *Nature*, 321(6073), p.832.
- 676 [39] Logan, G.A., Hayes, J.M., Hieshima, G.B. and Summons, R.E., 1995. Terminal Proterozoic reorganization of
677 biogeochemical cycles. *Nature*, 376(6535), p.53.
- 678 [40] Butterfield, N.J., 2009. Oxygen, animals and oceanic ventilation: an alternative view. *Geobiology*, 7(1), pp.1-7.
- 679 [41] Lenton, T.M., Boyle, R.A., Poulton, S.W., Shields-Zhou, G.A. and Butterfield, N.J., 2014. Co-evolution of
680 eukaryotes and ocean oxygenation in the Neoproterozoic era. *Nature Geoscience*, 7(4), p.257.
- 681 [42] Kennedy, M., Droser, M., Mayer, L.M., Pevear, D. and Mrofka, D., 2006. Late Precambrian oxygenation;
682 inception of the clay mineral factory. *Science*, 311(5766), pp.1446-1449.
- 683 [43] Knauth, L.P. and Kennedy, M.J., 2009. The late Precambrian greening of the Earth. *Nature*, 460(7256), p.728.
- 684 [44] Falkowski, P.G., Katz, M.E., Knoll, A.H., Quigg, A., Raven, J.A., Schofield, O. and Taylor, F.J.R., 2004. The
685 evolution of modern eukaryotic phytoplankton. *science*, 305(5682), pp.354-360.
- 686 [45] Steemans, P., Le Hérisse, A., Melvin, J., Miller, M.A., Paris, F., Verniers, J. and Wellman, C.H., 2009. Origin
687 and radiation of the earliest vascular land plants. *Science*, 324(5925), pp.353-353.
- 688 [46] Falkowski, P. and Knoll, A.H. eds., 2011. *Evolution of primary producers in the sea*. Academic Press.

- 689 [47] Shih, P.M., Wu, D., Latifi, A., Axen, S.D., Fewer, D.P., Talla, E., Calteau, A., Cai, F., De Marsac, N.T.,
690 Rippka, R. and Herdman, M., 2013. Improving the coverage of the cyanobacterial phylum using diversity-
691 driven genome sequencing. *Proceedings of the National Academy of Sciences*, 110(3), pp.1053-1058.
- 692 [48] Butterfield, N.J., 1997. Plankton ecology and the Proterozoic-Phanerozoic transition. *Paleobiology*, 23(2),
693 pp.247-262.
- 694 [49] Vidal, G. and Moczydłowska-Vidal, M., 1997. Biodiversity, speciation, and extinction trends of Proterozoic
695 and Cambrian phytoplankton. *Paleobiology*, 23(2), pp.230-246.
- 696 [50] Anbar, A.D. and Knoll, A.H., 2002. Proterozoic ocean chemistry and evolution: a bioinorganic bridge?
697 *Science*, 297(5584), pp.1137-1142.
- 698 [51] Knoll, A.H., Javaux, E.J., Hewitt, D. and Cohen, P., 2006. Eukaryotic organisms in Proterozoic
699 oceans. *Philosophical Transactions of the Royal Society of London B: Biological Sciences*, 361(1470), pp.1023-
700 1038.
- 701 [52] Brocks, J.J., Jarrett, A.J., Sirantoine, E., Hallmann, C., Hoshino, Y. and Liyanage, T., 2017. The rise of algae in
702 Cryogenian oceans and the emergence of animals. *Nature*, 548(7669), p.578.
- 703 [53] Isson, T.T., Love, G.D., Dupont, C.L., Reinhard, C.T., Zumberge, A.J., Asael, D., Gueguen, B., McCrow, J.,
704 Gill, B.C., Owens, J. and Rainbird, R.H., 2018. Tracking the rise of eukaryotes to ecological dominance with
705 zinc isotopes. *Geobiology*.
- 706 [54] Gueneli, N., McKenna, A.M., Ohkouchi, N., Boreham, C.J., Beghin, J., Javaux, E.J. and Brocks, J.J., 2018. 1.1-
707 billion-year-old porphyrins establish a marine ecosystem dominated by bacterial primary
708 producers. *Proceedings of the National Academy of Sciences*, p.201803866.
- 709 [55] Crockford, P.W., Hayles, J.A., Bao, H., Planavsky, N.J., Bekker, A., Fralick, P.W., Halverson, G.P., Bui, T.H.,
710 Peng, Y. and Wing, B.A., 2018. Triple oxygen isotope evidence for limited mid-Proterozoic primary
711 productivity. *Nature*, 559, pages613–616
- 712 [56] Waterbury, J.B., Watson, S.W., Guillard, R.R. and Brand, L.E., 1979. Widespread occurrence of a unicellular,
713 marine, planktonic, cyanobacterium. *Nature*, 277(5694), p.293.
- 714 [57] Chisholm, S.W., Olson, R.J., Zettler, E.R., Goericke, R., Waterbury, J.B. and Welschmeyer, N.A., 1988. A
715 novel free-living prochlorophyte abundant in the oceanic euphotic zone. *Nature*, 334(6180), p.340.
- 716 [58] Partensky, F., Hess, W.R. and Vaulot, D., 1999. Prochlorococcus, a marine photosynthetic prokaryote of global
717 significance. *Microbiology and molecular biology reviews*, 63(1), pp.106-127.
- 718 [59] Scanlan, D.J., Ostrowski, M., Mazard, S., Dufresne, A., Garczarek, L., Hess, W.R., Post, A.F., Hagemann, M.,
719 Paulsen, I. and Partensky, F., 2009. Ecological genomics of marine picocyanobacteria. *Microbiology and*
720 *Molecular Biology Reviews*, 73(2), pp.249-299.
- 721 [60] Sánchez-Baracaldo, P., Ridgwell, A. and Raven, J.A., 2014. A neoproterozoic transition in the marine nitrogen
722 cycle. *Current Biology*, 24(6), pp.652-657.
- 723 [61] Sánchez-Baracaldo, P., 2015. Origin of marine planktonic cyanobacteria. *Scientific reports*, 5, p.17418.
- 724 [62] Flombaum, P., Gallegos, J.L., Gordillo, R.A., Rincón, J., Zabala, L.L., Jiao, N., Karl, D.M., Li, W.K., Lomas,
725 M.W., Veneziano, D. and Vera, C.S., 2013. Present and future global distributions of the marine Cyanobacteria
726 Prochlorococcus and Synechococcus. *Proceedings of the National Academy of Sciences*, 110(24), pp.9824-
727 9829.
- 728 [63] Braakman, R., Follows, M.J. and Chisholm, S.W., 2017. Metabolic evolution and the self-organization of
729 ecosystems. *Proceedings of the National Academy of Sciences*, 114(14), E3091-E3100
- 730 [64] Valentine, J.W. and Moores, E.M., 1970. Plate-tectonic regulation of faunal diversity and sea level: a
731 model. *Nature*, 228(5272), p.657.
- 732 [65] Li, Z.X., Bogdanova, S.V., Collins, A.S., Davidson, A., De Waele, B., Ernst, R.E., Fitzsimons, I.C.W., Fuck,
733 R.A., Gladkochub, D.P., Jacobs, J. and Karlstrom, K.E., 2008. Assembly, configuration, and break-up history of
734 Rodinia: a synthesis. *Precambrian research*, 160(1-2), pp.179-210.
- 735 [66] Bradley, D.C., 2011. Secular trends in the geologic record and the supercontinent cycle. *Earth-Science*
736 *Reviews*, 108(1-2), pp.16-33.
- 737 [67] Liu, C., Knoll, A.H. and Hazen, R.M., 2017. Geochemical and mineralogical evidence that Rodinian assembly
738 was unique. *Nature communications*, 8(1), p.1950.
- 739 [68] De Roever, W.P., 1956. Some differences between post-Paleozoic and older regional metamorphism. *Geologie*
740 *en Mijnbouw*, 18, pp.123-127.
- 741 [69] Ernst, W.G., 1972. Occurrence and mineralogic evolution of blueschist belts with time. *American Journal of*
742 *Science*, 272(7), pp.657-668.
- 743 [70] Maruyama, S., Liou, J.G. and Terabayashi, M., 1996. Blueschists and eclogites of the world and their
744 exhumation. *International geology review*, 38(6), pp.485-594.

- 745 [71] Brown, M., 2007. Metamorphic conditions in orogenic belts: a record of secular change. *International Geology*
746 *Review*, 49(3), pp.193-234.
- 747 [72] Korenaga, J., 2013. Initiation and evolution of plate tectonics on Earth: theories and observations. *Annual*
748 *Review of Earth and Planetary Sciences*, 41, pp.117-151.
- 749 [73] Stern, R.J., Leybourne, M.I. and Tsujimori, T., 2016. Kimberlites and the start of plate
750 tectonics. *Geology*, 44(10), pp.799-802.
- 751 [74] Brown, M. and Johnson, T., 2018. Secular change in metamorphism and the onset of global plate
752 tectonics. *American Mineralogist*, 103(2), pp.181-196.
- 753 [75] Ronov, A.B., Khain, V.E., Balukhovskiy, A.N. and Seslavinsky, K.B., 1980. Quantitative analysis of
754 Phanerozoic sedimentation. *Sedimentary Geology*, 25(4), pp.311-325.
- 755 [76] Hallam, A., 1992. *Phanerozoic sea-level changes*. Columbia University Press.
- 756 [77] Peters, S.E. and Gaines, R.R., 2012. Formation of the 'Great Unconformity' as a trigger for the Cambrian
757 explosion. *Nature*, 484(7394), p.363.
- 758 [78] Rothman, D.H., Hayes, J.M. and Summons, R.E., 2003. Dynamics of the Neoproterozoic carbon
759 cycle. *Proceedings of the National Academy of Sciences*, 100(14), pp.8124-8129.
- 760 [79] Grotzinger, J.P., Fike, D.A. and Fischer, W.W., 2011. Enigmatic origin of the largest-known carbon isotope
761 excursion in Earth's history. *Nature Geoscience*, 4(5), p.285.
- 762 [80] Kirschvink, J.L., 1992. Late Proterozoic low-latitude global glaciation: the snowball Earth. The Proterozoic
763 Biosphere: A Multidisciplinary Study, eds Schopf JW, Klein C, Des Marais D (Cambridge Univ Press,
764 Cambridge, UK), pp 51–52.
- 765 [81] Hoffman, P.F., Kaufman, A.J., Halverson, G.P. and Schrag, D.P., 1998. A Neoproterozoic snowball
766 earth. *science*, 281(5381), pp.1342-1346.
- 767 [82] Pierrehumbert, R.T., Abbot, D.S., Voigt, A. and Koll, D., 2011. Climate of the Neoproterozoic. *Annual Review*
768 *of Earth and Planetary Sciences*, 39, pp.417-460.
- 769 [83] Hoffman, P.F., Abbot, D.S., Ashkenazy, Y., Benn, D.I., Brocks, J.J., Cohen, P.A., Cox, G.M., Creveling, J.R.,
770 Donnadieu, Y., Erwin, D.H. and Fairchild, I.J., 2017. Snowball Earth climate dynamics and Cryogenian
771 geology-geobiology. *Science Advances*, 3(11), p.e1600983.
- 772 [84] Canfield, D.E., 1998. A new model for Proterozoic ocean chemistry. *Nature*, 396(6710), p.450.
- 773 [85] Canfield, D.E., Poulton, S.W., Knoll, A.H., Narbonne, G.M., Ross, G., Goldberg, T. and Strauss, H., 2008.
774 Ferruginous conditions dominated later Neoproterozoic deep-water chemistry. *Science*, 321(5891), pp.949-952.
- 775 [86] Planavsky, N.J., McGoldrick, P., Scott, C.T., Li, C., Reinhard, C.T., Kelly, A.E., Chu, X., Bekker, A., Love,
776 G.D. and Lyons, T.W., 2011. Widespread iron-rich conditions in the mid-Proterozoic ocean. *Nature*, 477(7365),
777 p.448.
- 778 [87] Li, C., Love, G.D., Lyons, T.W., Fike, D.A., Sessions, A.L. and Chu, X., 2010. A stratified redox model for the
779 Ediacaran ocean. *Science*, 328(5974), pp.80-83.
- 780 [88] Sperling, E.A., Wolock, C.J., Morgan, A.S., Gill, B.C., Kunzmann, M., Halverson, G.P., Macdonald, F.A.,
781 Knoll, A.H. and Johnston, D.T., 2015. Statistical analysis of iron geochemical data suggests limited late
782 Proterozoic oxygenation. *Nature*, 523(7561), p.451.
- 783 [89] Lu, W., Ridgwell, A., Thomas, E., Hardisty, D.S., Luo, G., Algeo, T.J., Saltzman, M.R., Gill, B.C., Shen, Y.,
784 Ling, H.F. and Edwards, C.T., 2018. Late inception of a resiliently oxygenated upper ocean. *Science*,
785 p.eaar5372.
- 786 [90] Scott, C., Lyons, T.W., Bekker, A., Shen, Y.A., Poulton, S.W., Chu, X.L. and Anbar, A.D., 2008. Tracing the
787 stepwise oxygenation of the Proterozoic ocean. *Nature*, 452(7186), p.456.
- 788 [91] Chen, X., Ling, H.F., Vance, D., Shields-Zhou, G.A., Zhu, M., Poulton, S.W., Och, L.M., Jiang, S.Y., Li, D.,
789 Cremonese, L. and Archer, C., 2015. Rise to modern levels of ocean oxygenation coincided with the Cambrian
790 radiation of animals. *Nature communications*, 6, p.7142.
- 791 [92] Kunzmann, M., Bui, T.H., Crockford, P.W., Halverson, G.P., Scott, C., Lyons, T.W. and Wing, B.A., 2017.
792 Bacterial sulfur disproportionation constrains timing of Neoproterozoic oxygenation. *Geology*, 45(3), pp.207-
793 210.
- 794 [93] Fennel, K., Follows, M. and Falkowski, P.G., 2005. The co-evolution of the nitrogen, carbon and oxygen cycles
795 in the Proterozoic ocean. *American Journal of Science*, 305(6-8), pp.526-545.
- 796 [94] Zegeye, A., Bonneville, S., Benning, L.G., Sturm, A., Fowle, D.A., Jones, C., Canfield, D.E., Ruby, C.,
797 MacLean, L.C., Nomosatryo, S. and Crowe, S.A., 2012. Green rust formation controls nutrient availability in a
798 ferruginous water column. *Geology*, 40(7), pp.599-602.
- 799 [95] Laakso, T.A. and Schrag, D.P., 2014. Regulation of atmospheric oxygen during the Proterozoic. *Earth and*
800 *Planetary Science Letters*, 388, pp.81-91.

- 801 [96] Derry, L.A., 2015. Causes and consequences of mid-Proterozoic anoxia. *Geophysical Research Letters*, 42(20),
802 pp.8538-8546.
- 803 [97] Reinhard, C.T., Planavsky, N.J., Gill, B.C., Ozaki, K., Robbins, L.J., Lyons, T.W., Fischer, W.W., Wang, C.,
804 Cole, D.B. and Konhauser, K.O., 2017. Evolution of the global phosphorus cycle. *Nature*, 541(7637), p.386.
- 805 [98] Kipp, M.A. and Stüeken, E.E., 2017. Biomass recycling and Earth's early phosphorus cycle. *Science*
806 *advances*, 3(11), p.eaao4795.
- 807 [99] Jones, C., Nomosatryo, S., Crowe, S.A., Bjerrum, C.J. and Canfield, D.E., 2015. Iron oxides, divalent cations,
808 silica, and the early earth phosphorus crisis. *Geology*, 43(2), pp.135-138.
- 809 [100] Large, R.R., Halpin, J.A., Danyushevsky, L.V., Maslennikov, V.V., Bull, S.W., Long, J.A., Gregory, D.D.,
810 Lounejeva, E., Lyons, T.W., Sack, P.J. and McGoldrick, P.J., 2014. Trace element content of sedimentary pyrite
811 as a new proxy for deep-time ocean-atmosphere evolution. *Earth and Planetary Science Letters*, 389, pp.209-
812 220.
- 813 [101] Stüeken, E.E., 2013. A test of the nitrogen-limitation hypothesis for retarded eukaryote radiation: nitrogen
814 isotopes across a Mesoproterozoic basinal profile. *Geochimica et Cosmochimica Acta*, 120, pp.121-139.
- 815 [102] Kikumoto, R., Tahata, M., Nishizawa, M., Sawaki, Y., Maruyama, S., Shu, D., Han, J., Komiya, T., Takai, K.
816 and Ueno, Y., 2014. Nitrogen isotope chemostratigraphy of the Ediacaran and Early Cambrian platform
817 sequence at Three Gorges, South China. *Gondwana Research*, 25(3), pp.1057-1069.
- 818 [103] Ader, M., Sansjofre, P., Halverson, G.P., Busigny, V., Trindade, R.I., Kunzmann, M. and Nogueira, A.C.,
819 2014. Ocean redox structure across the Late Neoproterozoic Oxygenation Event: A nitrogen isotope
820 perspective. *Earth and Planetary Science Letters*, 396, pp.1-13.
- 821 [104] Wang, W., Guan, C., Zhou, C., Peng, Y., Pratt, L.M., Chen, X., Chen, L., Chen, Z., Yuan, X. and Xiao, S.,
822 2017. Integrated carbon, sulfur, and nitrogen isotope chemostratigraphy of the Ediacaran Lantian Formation in
823 South China: Spatial gradient, ocean redox oscillation, and fossil distribution. *Geobiology*, 15(4), pp.552-571.
- 824 [105] Koehler, M.C., Stüeken, E.E., Kipp, M.A., Buick, R. and Knoll, A.H., 2017. Spatial and temporal trends in
825 Precambrian nitrogen cycling: A Mesoproterozoic offshore nitrate minimum. *Geochimica et Cosmochimica*
826 *Acta*, 198, pp.315-337.
- 827 [106] Johnson, B.W., Poulton, S.W. and Goldblatt, C., 2017. Marine oxygen production and open water supported
828 an active nitrogen cycle during the Marinoan Snowball Earth. *Nature Communications*, 8(1), p.1316.
- 829 [107] Wang, X., Jiang, G., Shi, X., Peng, Y. and Morales, D., 2018. Nitrogen isotope constraints on the early
830 Ediacaran ocean redox structure. *Geochimica et Cosmochimica Acta*.
- 831 [108] Laakso, T.A. and Schrag, D.P., 2017. A theory of atmospheric oxygen. *Geobiology*, 15(3), pp.366-384.
- 832 [109] Raven, J.A., Evans, M.C. and Korb, R.E., 1999. The role of trace metals in photosynthetic electron transport
833 in O₂-evolving organisms. *Photosynthesis research*, 60(2-3), pp.111-150.
- 834 [110] Kuma, K., Nishioka, J. and Matsunaga, K., 1996. Controls on iron (III) hydroxide solubility in seawater: the
835 influence of pH and natural organic chelators. *Limnology and Oceanography*, 41(3), pp.396-407.
- 836 [111] Jolivet, J.P., Chanéac, C. and Tronc, E., 2004. Iron oxide chemistry. From molecular clusters to extended solid
837 networks. *Chemical Communications*, (5), pp.481-483.
- 838 [112] Saito, M.A., Sigman, D.M. and Morel, F.M., 2003. The bioinorganic chemistry of the ancient ocean: the co-
839 evolution of cyanobacterial metal requirements and biogeochemical cycles at the Archean-Proterozoic
840 boundary?. *Inorganica Chimica Acta*, 356, pp.308-318.
- 841 [113] Falkowski, P.G., 1997. Evolution of the nitrogen cycle and its influence on the biological sequestration of
842 CO₂ in the ocean. *Nature*, 387(6630), p.272.
- 843 [114] Dupont, C.L., Butcher, A., Valas, R.E., Bourne, P.E. and Caetano-Anollés, G., 2010. History of biological
844 metal utilization inferred through phylogenomic analysis of protein structures. *Proceedings of the National*
845 *Academy of Sciences*, 107(23), pp.10567-10572.
- 846 [115] Jelen, B.I., Giovannelli, D. and Falkowski, P.G., 2016. The role of microbial electron transfer in the
847 coevolution of the biosphere and geosphere. *Annual review of microbiology*, 70.
- 848 [116] Rue, E.L. and Bruland, K.W., 1995. Complexation of iron (III) by natural organic ligands in the Central North
849 Pacific as determined by a new competitive ligand equilibration/adsorptive cathodic stripping voltammetric
850 method. *Marine chemistry*, 50(1-4), pp.117-138.
- 851 [117] Gledhill, M. and Buck, K.N., 2012. The organic complexation of iron in the marine environment: a
852 review. *Frontiers in microbiology*, 3, p.69.
- 853 [118] Hassler, C.S., Schoemann, V., Nichols, C.M., Butler, E.C. and Boyd, P.W., 2011. Saccharides enhance iron
854 bioavailability to Southern Ocean phytoplankton. *Proceedings of the National Academy of Sciences*, 108(3),
855 pp.1076-1081.

- 856 [119] Roe, K.L. and Barbeau, K.A., 2014. Uptake mechanisms for inorganic iron and ferric citrate in
857 *Trichodesmium erythraeum* IMS101. *Metallomics*, 6(11), pp.2042-2051.
- 858 [120] Biller, S.J., Berube, P.M., Lindell, D. and Chisholm, S.W., 2015. Prochlorococcus: the structure and
859 function of collective diversity. *Nature Reviews Microbiology*, 13(1), p.13.
- 860 [121] Ralf, G. and Repeta, D.J., 1992. The pigments of Prochlorococcus marinus: The presence of
861 divinylchlorophyll a and b in a marine prokaryote. *Limnology and Oceanography*, 37(2), pp.425-433.
- 862 [122] Bibby, T.S., Nield, J., Partensky, F. and Barber, J., 2001. Oxyphotobacteria: Antenna ring around photosystem
863 I. *Nature*, 413(6856), p.590.
- 864 [123] Bibby, T.S., Mary, I., Nield, J., Partensky, F. and Barber, J., 2003. Low-light-adapted Prochlorococcus species
865 possess specific antennae for each photosystem. *Nature*, 424(6952), p.1051.
- 866 [124] Bailey, S., Melis, A., Mackey, K.R., Cardol, P., Finazzi, G., van Dijken, G., Berg, G.M., Arrigo, K., Shrager,
867 J. and Grossman, A., 2008. Alternative photosynthetic electron flow to oxygen in marine
868 *Synechococcus*. *Biochimica et Biophysica Acta (BBA)-Bioenergetics*, 1777(3), pp.269-276.
- 869 [125] Zorz, J.K., Allanach, J.R., Murphy, C.D., Roodvoets, M.S., Campbell, D.A. and Cockshutt, A.M., 2015. The
870 RUBISCO to photosystem II ratio limits the maximum photosynthetic rate in picocyanobacteria. *Life*, 5(1),
871 pp.403-417.
- 872 [126] Zinser, E.R., Lindell, D., Johnson, Z.I., Futschik, M.E., Steglich, C., Coleman, M.L., Wright, M.A., Rector,
873 T., Steen, R., McNulty, N. and Thompson, L.R., 2009. Choreography of the transcriptome, photophysiology,
874 and cell cycle of a minimal photoautotroph, Prochlorococcus. *PLoS one*, 4(4), p.e5135.
- 875 [127] Bertliss, S., Berglund, O., Pullin, M.J. and Chisholm, S.W., 2005. Release of dissolved organic matter by
876 Prochlorococcus. *Vie et Milieu*, 55(3-4), pp.225-232.
- 877 [128] Biddanda, B. and Benner, R., 1997. Carbon, nitrogen, and carbohydrate fluxes during the production of
878 particulate and dissolved organic matter by marine phytoplankton. *Limnology and Oceanography*, 42(3),
879 pp.506-518.
- 880 [129] Deng, W., Cruz, B.N. and Neuer, S., 2016. Effects of nutrient limitation on cell growth, TEP production and
881 aggregate formation of marine *Synechococcus*. *Aquatic Microbial Ecology*, 78(1), pp.39-49.
- 882 [130] Iuculano, F., Mazuecos, I.P., Reche, I. and Agustí, S., 2017. Prochlorococcus as a possible source for
883 transparent exopolymer particles (TEP). *Frontiers in microbiology*, 8, p.709.
- 884 [131] Tripp, H.J., Kitner, J.B., Schwalbach, M.S., Dacey, J.W., Wilhelm, L.J. and Giovannoni, S.J., 2008. SAR11
885 marine bacteria require exogenous reduced sulphur for growth. *Nature*, 452(7188), p.741.
- 886 [132] Carini, P., Steindler, L., Beszteri, S. and Giovannoni, S.J., 2013. Nutrient requirements for growth of the
887 extreme oligotroph 'Candidatus Pelagibacter ubique' HTCC1062 on a defined medium. *The ISME journal*, 7(3),
888 p.592.
- 889 [133] Frank, S.A., 1998. *Foundations of social evolution*. Princeton University Press.
- 890 [134] West, S.A., Griffin, A.S., Gardner, A. and Diggle, S.P., 2006. Social evolution theory for
891 microorganisms. *Nature Reviews Microbiology*, 4(8), p.597.
- 892 [135] Kashtan, N., Roggensack, S.E., Rodrigue, S., Thompson, J.W., Biller, S.J., Coe, A., Ding, H., Martinen, P.,
893 Malmstrom, R.R., Stocker, R. and Follows, M.J., 2014. Single-cell genomics reveals hundreds of coexisting
894 subpopulations in wild Prochlorococcus. *Science*, 344(6182), pp.416-420.
- 895 [136] Rankin, D.J., Bargum, K. and Kokko, H., 2007. The tragedy of the commons in evolutionary biology. *Trends*
896 *in ecology & evolution*, 22(12), pp.643-651.
- 897 [137] Kettler, G.C., Martiny, A.C., Huang, K., Zucker, J., Coleman, M.L., Rodrigue, S., Chen, F., Lapidus, A.,
898 Ferreira, S., Johnson, J. and Steglich, C., 2007. Patterns and implications of gene gain and loss in the evolution
899 of Prochlorococcus. *PLoS genetics*, 3(12), p.e231.
- 900 [138] Partensky, F. and Garczarek, L., 2009. Prochlorococcus: advantages and limits of minimalism. *Annual Review*
901 *of Marine Science*, 2, pp.305-331
- 902 [139] Di Cesare, A., Cabello-Yeves, P.J., Christmas, N.A., Sánchez-Baracaldo, P., Salcher, M.M. and Callieri, C.,
903 2018. Genome analysis of the freshwater planktonic *Vulcanococcus limneticus* sp. nov. reveals horizontal
904 transfer of nitrogenase operon and alternative pathways of nitrogen utilization. *BMC genomics*, 19(1), p.259.
- 905 [140] Angulo-Brown, F., Santillán, M. and Calleja-Quevedo, E., 1995. Thermodynamic optimality in some
906 biochemical reactions. *Il Nuovo Cimento D*, 17(1), pp.87-90.
- 907 [141] Waddell, T.G., Repovic, P., Meléndez-Hevia, E., Heinrich, R. and Montero, F., 1999. Optimization of
908 glycolysis: new discussions. *Biochemical education*, 27(1), pp.12-13.
- 909 [142] Pfeiffer, T., Schuster, S. and Bonhoeffer, S., 2001. Cooperation and competition in the evolution of ATP-
910 producing pathways. *Science*, 292(5516), pp.504-507.

- 911 [143] Molenaar, D., Van Berlo, R., De Ridder, D. and Teusink, B., 2009. Shifts in growth strategies reflect tradeoffs
912 in cellular economics. *Molecular systems biology*, 5(1), p.323.
- 913 [144] Flamholz, A., Noor, E., Bar-Even, A., Liebermeister, W. and Milo, R., 2013. Glycolytic strategy as a tradeoff
914 between energy yield and protein cost. *Proceedings of the National Academy of Sciences*, p.201215283.
- 915 [145] Basan, M., Hui, S., Okano, H., Zhang, Z., Shen, Y., Williamson, J.R. and Hwa, T., 2015. Overflow
916 metabolism in *Escherichia coli* results from efficient proteome allocation. *Nature*, 528(7580), p.99.
- 917 [146] Moore, L.R., Goericke, R. and Chisholm, S.W., 1995. Comparative physiology of *Synechococcus* and
918 *Prochlorococcus*: influence of light and temperature on growth, pigments, fluorescence and absorptive
919 properties. *Marine Ecology Progress Series*, pp.259-275.
- 920 [147] Neijssel, O.M. and Tempest, D.W., 1975. The regulation of carbohydrate metabolism in *Klebsiella aerogenes*
921 NCTC 418 organisms, growing in chemostat culture. *Archives of Microbiology*, 106(3), pp.251-258.
- 922 [148] Russell, J.B. and Cook, G.M., 1995. Energetics of bacterial growth: balance of anabolic and catabolic
923 reactions. *Microbiological reviews*, 59(1), pp.48-62.
- 924 [149] Dauner, M., Storni, T. and Sauer, U., 2001. *Bacillus subtilis* metabolism and energetics in carbon-limited and
925 excess-carbon chemostat culture. *Journal of bacteriology*, 183(24), pp.7308-7317.
- 926 [150] Vemuri, G.N., Eiteman, M.A., McEwen, J.E., Olsson, L. and Nielsen, J., 2007. Increasing NADH oxidation
927 reduces overflow metabolism in *Saccharomyces cerevisiae*. *Proceedings of the National Academy of*
928 *Sciences*, 104(7), pp.2402-2407.
- 929 [151] Bailey, S., Mann, N.H., Robinson, C. and Scanlan, D.J., 2005. The occurrence of rapidly reversible non-
930 photochemical quenching of chlorophyll a fluorescence in cyanobacteria. *FEBS letters*, 579(1), pp.275-280.
- 931 [152] Kulk, G., van de Poll, W.H., Visser, R.J. and Buma, A.G., 2011. Distinct differences in photoacclimation
932 potential between prokaryotic and eukaryotic oceanic phytoplankton. *Journal of Experimental Marine Biology*
933 *and Ecology*, 398(1-2), pp.63-72.
- 934 [153] Falkowski, P.G. and LaRoche, J., 1991. Acclimation to spectral irradiance in algae. *Journal of*
935 *Phycology*, 27(1), pp.8-14.
- 936 [154] Walters, R.G., 2005. Towards an understanding of photosynthetic acclimation. *Journal of experimental*
937 *botany*, 56(411), pp.435-447.
- 938 [155] Moore, L.R., Rocap, G. and Chisholm, S.W., 1998. Physiology and molecular phylogeny of coexisting
939 *Prochlorococcus* ecotypes. *Nature*, 393(6684), p.464.
- 940 [156] West, N.J. and Scanlan, D.J., 1999. Niche-partitioning of *Prochlorococcus* populations in a stratified water
941 column in the eastern North Atlantic Ocean. *Applied and environmental microbiology*, 65(6), pp.2585-2591.
- 942 [157] Johnson, Z.I., Zinser, E.R., Coe, A., McNulty, N.P., Woodward, E.M.S. and Chisholm, S.W., 2006. Niche
943 partitioning among *Prochlorococcus* ecotypes along ocean-scale environmental gradients. *Science*, 311(5768),
944 pp.1737-1740.
- 945 [158] Bouman, H.A., Ulloa, O., Scanlan, D.J., Zwirgmaier, K., Li, W.K., Platt, T., Stuart, V., Barlow, R., Leth, O.,
946 Clementson, L. and Lutz, V., 2006. Oceanographic basis of the global surface distribution of *Prochlorococcus*
947 ecotypes. *Science*, 312(5775), pp.918-921.
- 948 [159] Malmstrom, R.R., Coe, A., Kettler, G.C., Martiny, A.C., Frias-Lopez, J., Zinser, E.R. and Chisholm, S.W.,
949 2010. Temporal dynamics of *Prochlorococcus* ecotypes in the Atlantic and Pacific oceans. *The ISME*
950 *journal*, 4(10), p.1252.
- 951 [160] Morel, A., Ahn, Y.H., Partensky, F., Vaultot, D. and Claustre, H., 1993. *Prochlorococcus* and *Synechococcus*:
952 a comparative study of their optical properties in relation to their size and pigmentation. *Journal of Marine*
953 *Research*, 51(3), pp.617-649.
- 954 [161] Lynch, M. and Conery, J.S., 2003. The origins of genome complexity. *science*, 302(5649), pp.1401-1404.
- 955 [162] Giovannoni, S.J., Tripp, H.J., Givan, S., Podar, M., Vergin, K.L., Baptista, D., Bibbs, L., Eads, J., Richardson,
956 T.H., Noordewier, M. and Rappé, M.S., 2005. Genome streamlining in a cosmopolitan oceanic
957 bacterium. *science*, 309(5738), pp.1242-1245.
- 958 [163] Giovannoni, S.J., Thrash, J.C. and Temperton, B., 2014. Implications of streamlining theory for microbial
959 ecology. *The ISME journal*, 8(8), p.1553.
- 960 [164] Moore, C.M., Mills, M.M., Arrigo, K.R., Berman-Frank, I., Bopp, L., Boyd, P.W., Galbraith, E.D., Geider,
961 R.J., Guieu, C., Jaccard, S.L. and Jickells, T.D., 2013. Processes and patterns of oceanic nutrient
962 limitation. *Nature Geoscience*, 6(9), p.701.
- 963 [165] Dufresne, A., Garczarek, L. and Partensky, F., 2005. Accelerated evolution associated with genome reduction
964 in a free-living prokaryote. *Genome biology*, 6(2), p.R14.
- 965 [166] Grzymalski, J.J. and Dussaq, A.M., 2012. The significance of nitrogen cost minimization in proteomes of
966 marine microorganisms. *The ISME journal*, 6(1), p.71.

- 967 [167] Van Mooy, B.A., Rocap, G., Fredricks, H.F., Evans, C.T. and Devol, A.H., 2006. Sulfolipids dramatically
968 decrease phosphorus demand by picocyanobacteria in oligotrophic marine environments. *Proceedings of the*
969 *National Academy of Sciences*, 103(23), pp.8607-8612.
- 970 [168] Van Mooy, B.A., Fredricks, H.F., Pedler, B.E., Dyhrman, S.T., Karl, D.M., Koblížek, M., Lomas, M.W.,
971 Mincer, T.J., Moore, L.R., Moutin, T. and Rappé, M.S., 2009. Phytoplankton in the ocean use non-phosphorus
972 lipids in response to phosphorus scarcity. *Nature*, 458(7234), p.69.
- 973 [169] Button, D.K., 1991. Biochemical basis for whole-cell uptake kinetics: specific affinity, oligotrophic capacity,
974 and the meaning of the Michaelis constant. *Applied and Environmental Microbiology*, 57(7), pp.2033-2038.
- 975 [170] Duff, S.M., Moorhead, G.B., Lefebvre, D.D. and Plaxton, W.C., 1989. Phosphate starvation inducible
976 bypasses' of adenylate and phosphate dependent glycolytic enzymes in *Brassica nigra* suspension cells. *Plant*
977 *Physiology*, 90(4), pp.1275-1278.
- 978 [171] Theodorou, M.E., Elrifi, I.R., Turpin, D.H. and Plaxton, W.C., 1991. Effects of phosphorus limitation on
979 respiratory metabolism in the green alga *Selenastrum minutum*. *Plant Physiology*, 95(4), pp.1089-1095.
- 980 [172] Bulthuis, B.A., Koningstein, G.M., Stouthamer, A.H. and van Verseveld, H.W., 1993. The relation of proton
981 motive force, adenylate energy charge and phosphorylation potential to the specific growth rate and efficiency
982 of energy transduction in *Bacillus licheniformis* under aerobic growth conditions. *Antonie Van*
983 *Leeuwenhoek*, 63(1), pp.1-16.
- 984 [173] Gauthier, D.A. and Turpin, D.H., 1994. Inorganic phosphate (Pi) enhancement of dark respiration in the Pi-
985 limited green alga *Selenastrum minutum* (interactions between H⁺/Pi cotransport, the plasmalemma H⁺-
986 ATPase, and dark respiratory carbon flow). *Plant physiology*, 104(2), pp.629-637.
- 987 [174] Neijssel, O.M. and Tempest, D.W., 1976. The role of energy-spilling reactions in the growth of *Klebsiella*
988 *aerogenes* NCTC 418 in aerobic chemostat culture. *Archives of microbiology*, 110(2-3), pp.305-311.
- 989 [175] Vander Heiden, M.G., Cantley, L.C. and Thompson, C.B., 2009. Understanding the Warburg effect: the
990 metabolic requirements of cell proliferation. *science*, 324(5930), pp.1029-1033.
- 991 [176] Fogg, G.E., 1983. The ecological significance of extracellular products of phytoplankton
992 photosynthesis. *Botanica marina*, 26(1), pp.3-14.
- 993 [177] Myklesstad, S.M., 1995. Release of extracellular products by phytoplankton with special emphasis on
994 polysaccharides. *Science of the total Environment*, 165(1-3), pp.155-164.
- 995 [178] Alcoverro, T., Conte, E. and Mazzella, L., 2000. Production of mucilage by the Adriatic epipellic diatom
996 *Cylindrotheca closterium* (Bacillariophyceae) under nutrient limitation. *Journal of Phycology*, 36(6), pp.1087-
997 1095.
- 998 [179] Staats, N., Stal, L.J. and Mur, L.R., 2000. Exopolysaccharide production by the epipellic diatom *Cylindrotheca*
999 *closterium*: effects of nutrient conditions. *Journal of Experimental Marine Biology and Ecology*, 249(1), pp.13-
1000 27.
- 1001 [180] Wetz, M.S. and Wheeler, P.A., 2007. Release of dissolved organic matter by coastal diatoms. *Limnology and*
1002 *Oceanography*, 52(2), pp.798-807.
- 1003 [181] Beard, D.A. and Qian, H., 2007. Relationship between thermodynamic driving force and one-way fluxes in
1004 reversible processes. *PloS one*, 2(1), p.e144.
- 1005 [182] Hansell, D.A., Carlson, C.A., Repeta, D.J. and Schlitzer, R., 2009. Dissolved organic matter in the ocean: A
1006 controversy stimulates new insights. *Oceanography*, 22(4), pp.202-211.
- 1007 [183] Berube, P.M., Rasmussen, A., Braakman, R., Stepanauskas, R. and Chisholm, S.W., 2018. Emergence of trait
1008 variability through the lens of nitrogen assimilation in *Prochlorococcus*. *bioRxiv*, p.383927.
- 1009 [184] Berube, P.M., Coe, A., Roggensack, S.E. and Chisholm, S.W., 2016. Temporal dynamics of *Prochlorococcus*
1010 cells with the potential for nitrate assimilation in the subtropical Atlantic and Pacific oceans. *Limnology and*
1011 *Oceanography*, 61(2), pp.482-495.
- 1012 [185] Sunda, W.G. and Huntsman, S.A., 1997. Interrelated influence of iron, light and cell size on marine
1013 phytoplankton growth. *Nature*, 390(6658), p.389.
- 1014 [186] Strzepek, R.F. and Harrison, P.J., 2004. Photosynthetic architecture differs in coastal and oceanic
1015 diatoms. *Nature*, 431(7009), p.689.
- 1016 [187] Cardol, P., Bailleul, B., Rappaport, F., Derelle, E., Béal, D., Breyton, C., Bailey, S., Wollman, F.A.,
1017 Grossman, A., Moreau, H. and Finazzi, G., 2008. An original adaptation of photosynthesis in the marine green
1018 alga *Ostreococcus*. *Proceedings of the National Academy of Sciences*, 105(22), pp.7881-7886.
- 1019 [188] Banfield, J.F., Barker, W.W., Welch, S.A. and Taunton, A., 1999. Biological impact on mineral dissolution:
1020 application of the lichen model to understanding mineral weathering in the rhizosphere. *Proceedings of the*
1021 *National Academy of Sciences*, 96(7), pp.3404-3411.

- 1022 [189] Uroz, S., Calvaruso, C., Turpault, M.P. and Frey-Klett, P., 2009. Mineral weathering by bacteria: ecology,
1023 actors and mechanisms. *Trends in microbiology*, 17(8), pp.378-387.
- 1024 [190] Jickells, T.D., An, Z.S., Andersen, K.K., Baker, A.R., Bergametti, G., Brooks, N., Cao, J.J., Boyd, P.W.,
1025 Duce, R.A., Hunter, K.A. and Kawahata, H., 2005. Global iron connections between desert dust, ocean
1026 biogeochemistry, and climate. *science*, 308(5718), pp.67-71.
- 1027 [191] Benitez-Nelson, C.R., 2000. The biogeochemical cycling of phosphorus in marine systems. *Earth-Science*
1028 *Reviews*, 51(1-4), pp.109-135.
- 1029 [192] Ridame, C. and Guieu, C., 2002. Saharan input of phosphate to the oligotrophic water of the open western
1030 Mediterranean Sea. *Limnology and Oceanography*, 47(3), pp.856-869.
- 1031 [193] Romano, S., Bondarev, V., Kölling, M., Dittmar, T. and Schulz-Vogt, H.N., 2017. Phosphate limitation
1032 triggers the dissolution of precipitated iron by the marine bacterium *Pseudovibrio* sp. FO-BEG1. *Frontiers in*
1033 *microbiology*, 8, p.364.
- 1034 [194] Tyrrell, T., 1999. The relative influences of nitrogen and phosphorus on oceanic primary
1035 production. *Nature*, 400(6744), p.525.
- 1036 [195] Vitousek, P.M., Cassman, K.E.N., Cleveland, C., Crews, T., Field, C.B., Grimm, N.B., Howarth, R.W.,
1037 Marino, R., Martinelli, L., Rastetter, E.B. and Sprent, J.I., 2002. Towards an ecological understanding of
1038 biological nitrogen fixation. In *The Nitrogen Cycle at Regional to Global Scales* (pp. 1-45). Springer,
1039 Dordrecht.
- 1040 [196] Mills, M.M., Ridame, C., Davey, M., La Roche, J. and Geider, R.J., 2004. Iron and phosphorus co-limit
1041 nitrogen fixation in the eastern tropical North Atlantic. *Nature*, 429(6989), p.292.
- 1042 [197] Petitjean, C., Moreira, D., López-García, P. and Brochier-Armanet, C., 2012. Horizontal gene transfer of a
1043 chloroplast DnaJ-Fer protein to Thaumarchaeota and the evolutionary history of the DnaK chaperone system in
1044 Archaea. *BMC evolutionary biology*, 12(1), p.226.
- 1045 [198] Gubry-Rangin, C., Kratsch, C., Williams, T.A., McHardy, A.C., Embley, T.M., Prosser, J.I. and Macqueen,
1046 D.J., 2015. Coupling of diversification and pH adaptation during the evolution of terrestrial
1047 Thaumarchaeota. *Proceedings of the National Academy of Sciences*, 112(30), pp.9370-9375.
- 1048 [199] Morris, R.M., Rappé, M.S., Connon, S.A., Vergin, K.L., Siebold, W.A., Carlson, C.A. and Giovannoni, S.J.,
1049 2002. SAR11 clade dominates ocean surface bacterioplankton communities. *Nature*, 420(6917), p.806.
- 1050 [200] Luo, H., Csúros, M., Hughes, A.L. and Moran, M.A., 2013. Evolution of divergent life history strategies in
1051 marine alphaproteobacteria. *MBio*, 4(4), pp.e00373-13.
- 1052 [201] Schwalbach, M.S., Tripp, H.J., Steindler, L., Smith, D.P. and Giovannoni, S.J., 2010. The presence of the
1053 glycolysis operon in SAR11 genomes is positively correlated with ocean productivity. *Environmental*
1054 *microbiology*, 12(2), pp.490-500.
- 1055 [202] Partensky, F., La Roche, J., Wyman, K. and Falkowski, P.G., 1997. The divinyl-chlorophyll a/b-protein
1056 complexes of two strains of the oxyphototrophic marine prokaryote *Prochlorococcus*—characterization and
1057 response to changes in growth irradiance. *Photosynthesis research*, 51(3), pp.209-222.
- 1058 [203] Melis, A. and Brown, J.S., 1980. Stoichiometry of system I and system II reaction centers and of
1059 plastoquinone in different photosynthetic membranes. *Proceedings of the National Academy of Sciences*, 77(8),
1060 pp.4712-4716.
- 1061 [204] McDonald, A.E. and Vanlerberghe, G.C., 2005. Alternative oxidase and plastoquinol terminal oxidase in
1062 marine prokaryotes of the Sargasso Sea. *Gene*, 349, pp.15-24.
- 1063 [205] Noctor, G., De Paepe, R. and Foyer, C.H., 2007. Mitochondrial redox biology and homeostasis in
1064 plants. *Trends in plant science*, 12(3), pp.125-134.
- 1065 [206] Morris, J.J., Kirkegaard, R., Szul, M.J., Johnson, Z.I. and Zinser, E.R., 2008. Facilitation of robust growth of
1066 *Prochlorococcus* colonies and dilute liquid cultures by “helper” heterotrophic bacteria. *Applied and*
1067 *environmental microbiology*, 74(14), pp.4530-4534.
- 1068 [207] Morris, J.J., Johnson, Z.I., Szul, M.J., Keller, M. and Zinser, E.R., 2011. Dependence of the cyanobacterium
1069 *Prochlorococcus* on hydrogen peroxide scavenging microbes for growth at the ocean's surface. *PloS one*, 6(2),
1070 p.e16805.
- 1071 [208] Butterfield, N.J., Knoll, A.H. and Swett, K., 1988. Exceptional preservation of fossils in an Upper Proterozoic
1072 shale. *Nature*, 334(6181), p.424.
- 1073 [209] Douzery, E.J., Snell, E.A., Bapteste, E., Delsuc, F. and Philippe, H., 2004. The timing of eukaryotic evolution:
1074 does a relaxed molecular clock reconcile proteins and fossils?. *Proceedings of the National Academy of*
1075 *Sciences*, 101(43), pp.15386-15391.
- 1076 [210] Yoon, H.S., Hackett, J.D., Ciniglia, C., Pinto, G. and Bhattacharya, D., 2004. A molecular timeline for the
1077 origin of photosynthetic eukaryotes. *Molecular biology and evolution*, 21(5), pp.809-818.

- 1078 [211] Parfrey, L.W., Lahr, D.J., Knoll, A.H. and Katz, L.A., 2011. Estimating the timing of early eukaryotic
1079 diversification with multigene molecular clocks. *Proceedings of the National Academy of Sciences*, 108(33),
1080 pp.13624-13629.
- 1081 [212] Ryan, P.R., Delhaize, E. and Jones, D.L., 2001. Function and mechanism of organic anion exudation from
1082 plant roots. *Annual review of plant biology*, 52(1), pp.527-560.
- 1083 [213] Dakora, F.D. and Phillips, D.A., 2002. Root exudates as mediators of mineral acquisition in low-nutrient
1084 environments. In *Food Security in Nutrient-Stressed Environments: Exploiting Plants' Genetic Capabilities* (pp.
1085 201-213). Springer, Dordrecht.
- 1086 [214] Soltis, D.E., Soltis, P.S., Morgan, D.R., Swensen, S.M., Mullin, B.C., Dowd, J.M. and Martin, P.G., 1995.
1087 Chloroplast gene sequence data suggest a single origin of the predisposition for symbiotic nitrogen fixation in
1088 angiosperms. *Proceedings of the National Academy of Sciences*, 92(7), pp.2647-2651.
- 1089 [215] Gruber, N. and Galloway, J.N., 2008. An Earth-system perspective of the global nitrogen
1090 cycle. *Nature*, 451(7176), p.293.
- 1091 [216] Berner, R.A. and Canfield, D.E., 1989. A new model for atmospheric oxygen over Phanerozoic
1092 time. *American Journal of Science*, 289(4), pp.333-361.
- 1093 [217] Berner, R.A., 2006. GEOCARBSULF: a combined model for Phanerozoic atmospheric O₂ and
1094 CO₂. *Geochimica et Cosmochimica Acta*, 70(23), pp.5653-5664.
- 1095 [218] Braakman, R. and Smith, E., 2012. The compositional and evolutionary logic of metabolism. *Physical*
1096 *biology*, 10(1), p.011001.
- 1097 [219] Sanchez-Baracaldo, P., Hayes, P.K. and BLANK, C.E., 2005. Morphological and habitat evolution in the
1098 Cyanobacteria using a compartmentalization approach. *Geobiology*, 3(3), pp.145-165.
- 1099 [220] Sánchez-Baracaldo, P., Raven, J.A., Pisani, D. and Knoll, A.H., 2017. Early photosynthetic eukaryotes
1100 inhabited low-salinity habitats. *Proceedings of the National Academy of Sciences*, 114(37), pp.E7737-E7745.
- 1101 [221] Schidlowski, M., Eichmann, R. and Junge, C.E., 1976. Carbon isotope geochemistry of the Precambrian
1102 Lomagundi carbonate province, Rhodesia. *Geochimica et Cosmochimica Acta*, 40(4), pp.449-455.
- 1103 [222] Karhu, J.A. and Holland, H.D., 1996. Carbon isotopes and the rise of atmospheric oxygen. *Geology*, 24(10),
1104 pp.867-870.
- 1105 [223] Evans, D.A., Beukes, N.J. and Kirschvink, J.L., 1997. Low-latitude glaciation in the Palaeoproterozoic
1106 era. *Nature*, 386(6622), p.262.
- 1107 [224] Williams, G.E. and Schmidt, P.W., 1997. Paleomagnetism of the Paleoproterozoic Gowganda and Lorrain
1108 formations, Ontario: low paleolatitude for Huronian glaciation. *Earth and Planetary Science Letters*, 153(3-4),
1109 pp.157-169.
- 1110 [225] Kirschvink, J.L., Gaidos, E.J., Bertani, L.E., Beukes, N.J., Gutzmer, J., Maepa, L.N. and Steinberger, R.E.,
1111 2000. Paleoproterozoic snowball Earth: Extreme climatic and geochemical global change and its biological
1112 consequences. *Proceedings of the National Academy of Sciences*, 97(4), pp.1400-1405.
- 1113 [226] Kopp, R.E., Kirschvink, J.L., Hilburn, I.A. and Nash, C.Z., 2005. The Paleoproterozoic snowball Earth: a
1114 climate disaster triggered by the evolution of oxygenic photosynthesis. *Proceedings of the National Academy of*
1115 *Sciences*, 102(32), pp.11131-11136.
- 1116 [227] Gumsley, A.P., Chamberlain, K.R., Bleeker, W., Söderlund, U., de Kock, M.O., Larsson, E.R. and Bekker, A.,
1117 2017. Timing and tempo of the Great Oxidation Event. *Proceedings of the National Academy of*
1118 *Sciences*, 114(8), pp.1811-1816.
- 1119 [228] Brown, M., 2006. Duality of thermal regimes is the distinctive characteristic of plate tectonics since the
1120 Neoproterozoic. *Geology*, 34(11), pp.961-964.
- 1121 [229] Cawood, P.A., Kroner, A. and Pisarevsky, S., 2006. Precambrian plate tectonics: criteria and evidence. *GSA*
1122 *today*, 16(7), p.4.
- 1123 [230] Condie, K.C. and Kröner, A., 2008. When did plate tectonics begin? Evidence from the geologic record.
1124 In *When did plate tectonics begin on planet Earth* (Vol. 440, pp. 281-294). Geological Society of America
1125 Special Papers.
- 1126 [231] Keller, C.B. and Schoene, B., 2012. Statistical geochemistry reveals disruption in secular lithospheric
1127 evolution about 2.5 Gyr ago. *Nature*, 485(7399), p.490.
- 1128 [232] Cawood, P.A., Hawkesworth, C.J., Pisarevsky, S.A., Dhuime, B., Capitanio, F.A., Nebel, O., 2018.
1129 Geological archive of the onset of plate tectonics. *Philosophical Transactions of the Royal Society A*, 378,
1130 20170405
- 1131 [233] Blank, C.E. and Sanchez-Baracaldo, P., 2010. Timing of morphological and ecological innovations in the
1132 cyanobacteria—a key to understanding the rise in atmospheric oxygen. *Geobiology*, 8(1), pp.1-23.

- 1133 [234] Shih, P.M. and Matzke, N.J., 2013. Primary endosymbiosis events date to the later Proterozoic with cross-
1134 calibrated phylogenetic dating of duplicated ATPase proteins. *Proceedings of the National Academy of*
1135 *Sciences*, 110(30), pp.12355-12360.
- 1136 [235] Schirmer, B.E., Gugger, M. and Donoghue, P.C., 2015. Cyanobacteria and the Great Oxidation Event:
1137 evidence from genes and fossils. *Palaeontology*, 58(5), pp.769-785.
- 1138 [236] Shih, P.M., Hemp, J., Ward, L.M., Matzke, N.J. and Fischer, W.W., 2017. Crown group Oxyphotobacteria
1139 postdate the rise of oxygen. *Geobiology*, 15(1), pp.19-29.
- 1140 [237] Gibson, T.M., Shih, P.M., Cumming, V.M., Fischer, W.W., Crockford, P.W., Hodgskiss, M.S., Wörndle, S.,
1141 Creaser, R.A., Rainbird, R.H., Skulski, T.M. and Halverson, G.P., 2017. Precise age of *Bangiomorpha*
1142 *pubescens* dates the origin of eukaryotic photosynthesis. *Geology*, 46(2), pp.135-138.
- 1143 [238] Magnabosco, C., Moore, K.R., Wolfe, J.M. and Fournier, G.P., 2018. Dating phototrophic microbial lineages
1144 with reticulate gene histories. *Geobiology*, 16(2), pp.179-189.
- 1145 [239] Anbar, A.D., Duan, Y., Lyons, T.W., Arnold, G.L., Kendall, B., Creaser, R.A., Kaufman, A.J., Gordon, G.W.,
1146 Scott, C., Garvin, J. and Buick, R., 2007. A whiff of oxygen before the great oxidation
1147 event?. *Science*, 317(5846), pp.1903-1906.
- 1148 [240] Bosak, T., Liang, B., Sim, M.S. and Petroff, A.P., 2009. Morphological record of oxygenic photosynthesis in
1149 conical stromatolites. *Proceedings of the National Academy of Sciences*, 106(27), pp.10939-10943.
- 1150 [241] Farquhar, J., Zerkle, A.L. and Bekker, A., 2011. Geological constraints on the origin of oxygenic
1151 photosynthesis. *Photosynthesis research*, 107(1), pp.11-36.
- 1152 [242] Schirmer, B.E., de Vos, J.M., Antonelli, A. and Bagheri, H.C., 2013. Evolution of multicellularity
1153 coincided with increased diversification of cyanobacteria and the Great Oxidation Event. *Proceedings of the*
1154 *National Academy of Sciences*, 110(5), pp.1791-1796.
- 1155 [243] Crowe, S.A., Døssing, L.N., Beukes, N.J., Bau, M., Kruger, S.J., Frei, R. and Canfield, D.E., 2013.
1156 Atmospheric oxygenation three billion years ago. *Nature*, 501(7468), p.535.
- 1157 [244] Planavsky, N.J., Asael, D., Hofmann, A., Reinhard, C.T., Lalonde, S.V., Knudsen, A., Wang, X., Ossa, F.O.,
1158 Pecoits, E., Smith, A.J. and Beukes, N.J., 2014. Evidence for oxygenic photosynthesis half a billion years
1159 before the Great Oxidation Event. *Nature Geoscience*, 7(4), p.283.
- 1160 [245] Wang, X., Planavsky, N.J., Hofmann, A., Saupe, E.E., De Corte, B.P., Philippot, P., LaLonde, S.V., Jemison,
1161 N.E., Zou, H., Ossa, F.O. and Rybacki, K., 2018. A Mesoarchean shift in uranium isotope
1162 systematics. *Geochimica et Cosmochimica Acta*, 238, pp.438-452.
- 1163 [246] Cardona, T., Sanchez-Baracaldo, P., Rutherford, A.W., Larkum, A.W.D., 2018. Early Archean origin of
1164 Photosystem II. *BioRxiv*, 109447
- 1165 [247] Arndt, N., 1999. Why was flood volcanism on submerged continental platforms so common in the
1166 Precambrian?. *Precambrian Research*, 97(3-4), pp.155-164.
- 1167 [248] Flament, N., Coltice, N. and Rey, P.F., 2008. A case for late-Archaeon continental emergence from thermal
1168 evolution models and hypsometry. *Earth and Planetary Science Letters*, 275(3-4), pp.326-336.
- 1169 [249] Korenaga, J., Planavsky, N.J. and Evans, D.A., 2017. Global water cycle and the coevolution of the Earth's
1170 interior and surface environment. *Phil. Trans. R. Soc. A*, 375(2094), p.20150393.
- 1171 [250] Raymond, J. and Segrè, D., 2006. The effect of oxygen on biochemical networks and the evolution of complex
1172 life. *Science*, 311(5768), pp.1764-1767.
- 1173 [251] Hohmann-Marriott, M.F. and Blankenship, R.E., 2011. Evolution of photosynthesis. *Annual review of plant*
1174 *biology*, 62, pp.515-548.
- 1175 [252] Cardona, T., Murray, J.W. and Rutherford, A.W., 2015. Origin and evolution of water oxidation before the
1176 last common ancestor of the cyanobacteria. *Molecular biology and evolution*, 32(5), pp.1310-1328.
- 1177 [253] Fischer, W.W., Hemp, J. and Valentine, J.S., 2016. How did life survive Earth's great oxygenation? *Current*
1178 *opinion in chemical biology*, 31, pp.166-178.
- 1179 [254] Soo, R.M., Hemp, J., Parks, D.H., Fischer, W.W. and Hugenholtz, P., 2017. On the origins of oxygenic
1180 photosynthesis and aerobic respiration in Cyanobacteria. *Science*, 355(6332), pp.1436-1440.
- 1181 [255] Kacar, B., Hanson-Smith, V., Adam, Z.R. and Boekelheide, N., 2017. Constraining the timing of the Great
1182 Oxidation Event within the Rubisco phylogenetic tree. *Geobiology*, 15(5), pp.628-640.
- 1183 [256] Mloszewski, A.M., Cole, D.B., Planavsky, N.J., Kappler, A., Whitford, D.S., Owttrim, G.W. and Konhauser,
1184 K.O., 2018. UV radiation limited the expansion of cyanobacteria in early marine photic environments. *Nature*
1185 *communications*, 9(1), p.3088.
- 1186 [257] Rosing, M.T., Bird, D.K., Sleep, N.H., Glassley, W. and Albarede, F., 2006. The rise of continents—an essay
1187 on the geologic consequences of photosynthesis. *Palaeogeography, Palaeoclimatology, Palaeoecology*, 232(2-
1188 4), pp.99-113.

- 1189 [258] Lee, C.T.A., Morton, D.M., Little, M.G., Kistler, R., Horodyskyj, U.N., Leeman, W.P. and Agranier, A., 2008.
1190 Regulating continent growth and composition by chemical weathering. *Proceedings of the National Academy of*
1191 *Sciences*, 105(13), pp.4981-4986.
- 1192 [259] Sleep, N.H., Bird, D.K. and Pope, E., 2012. Paleontology of Earth's mantle. *Annual Review of Earth and*
1193 *Planetary Sciences*, 40, pp.277-300.
- 1194 [260] Höning, D., Hansen-Goos, H., Airo, A. and Spohn, T., 2014. Biotic vs. abiotic Earth: A model for mantle
1195 hydration and continental coverage. *Planetary and Space Science*, 98, pp.5-13.
- 1196 [261] Höning, D. and Spohn, T., 2016. Continental growth and mantle hydration as intertwined feedback cycles in
1197 the thermal evolution of Earth. *Physics of the Earth and Planetary Interiors*, 255, pp.27-49.
- 1198 [262] Maruyama, S. and Liou, J.G., 2005. From snowball to Phanerozoic Earth. *International Geology*
1199 *Review*, 47(8), pp.775-791.
- 1200 [263] Lee, C.T.A., Caves, J., Jiang, H., Cao, W., Lenardic, A., McKenzie, N.R., Shorttle, O., Yin, Q.Z. and Dyer, B.,
1201 2018. Deep mantle roots and continental emergence: implications for whole-Earth elemental cycling, long-term
1202 climate, and the Cambrian explosion. *International Geology Review*, 60(4), pp.431-448.
- 1203 [264] Berner, R.A., 1992. Weathering, plants, and the long-term carbon cycle. *Geochimica et Cosmochimica*
1204 *Acta*, 56(8), pp.3225-3231.
- 1205 [265] Berner, R.A., 1997. The rise of plants and their effect on weathering and atmospheric
1206 CO₂. *Science*, 276(5312), pp.544-546.
- 1207 [266] Lenton, T.M., Crouch, M., Johnson, M., Pires, N. and Dolan, L., 2012. First plants cooled the
1208 Ordovician. *Nature Geoscience*, 5(2), p.86.
- 1209 [267] Boyce, C.K. and Lee, J.E., 2017. Plant evolution and climate over geological timescales. *Annual Review of*
1210 *Earth and Planetary Sciences*, 45, pp.61-87.
- 1211 [268] Husson, J.M. and Peters, S.E., 2017. Atmospheric oxygenation driven by unsteady growth of the continental
1212 sedimentary reservoir. *Earth and Planetary Science Letters*, 460, pp.68-75.
- 1213 [269] Peters, S.E. and Husson, J.M., 2017. Sediment cycling on continental and oceanic crust. *Geology*, 45(4),
1214 pp.323-326.
- 1215 [270] Hartnett, H.E., Keil, R.G., Hedges, J.I. and Devol, A.H., 1998. Influence of oxygen exposure time on organic
1216 carbon preservation in continental margin sediments. *Nature*, 391(6667), p.572.
- 1217 [271] Tosca, N.J., Johnston, D.T., Mushegian, A., Rothman, D.H., Summons, R.E. and Knoll, A.H., 2010. Clay
1218 mineralogy, organic carbon burial, and redox evolution in Proterozoic oceans. *Geochimica et Cosmochimica*
1219 *Acta*, 74(5), pp.1579-1592.
- 1220 [272] Hazen, R.M., Sverjensky, D.A., Azzolini, D., Bish, D.L., Elmore, S.C., Hinnov, L. and Milliken, R.E., 2013.
1221 Clay mineral evolution. *American Mineralogist*, 98(11-12), pp.2007-2029.
- 1222 [273] McMahon, W.J. and Davies, N.S., 2018. Evolution of alluvial mudrock forced by early land
1223 plants. *Science*, 359(6379), pp.1022-1024.